

Bicyclic Boronate VNRX-5133 Inhibits Metallo- and Serine- β -Lactamases

SUPPORTING INFORMATION

Alen Krajnc^a, Jürgen Brem^a, Philip Hinchliffe^b, Karina Calvopiña^a, Tharindi D. Panduwawala^a, Pauline A. Lang^a, Jos J. A. G. Kamps^a, Jonathan M. Tyrrell^c, Emma Widlake^c, Benjamin G. Saward^a, Timothy R. Walsh^c, James Spencer^b and Christopher J. Schofield^{a,}.*

^aChemistry Research Laboratory, Department of Chemistry, 12 Mansfield Road, University of Oxford, Oxford, OX1 3TA, United Kingdom.

^bSchool of Cellular and Molecular Medicine, Biomedical Sciences Building, University Walk, University of Bristol, Bristol, BS8 1TD, United Kingdom.

^cDepartment of Medical Microbiology & Infectious Disease, Institute of Infection & Immunity, UHW Main Building, Heath Park, Cardiff, CF14 4XN, United Kingdom.

CONTENTS

Figure S1. Comparison of the binding modes of VNRX-5133 and benzylpenicillin.....	S3
Figure S2. Crystal structure views of the tricyclic forms of VNRX-5133 in complex with NDM-1	S4
Figure S3. View of the overall fold of the class D serine- β -lactamase (SBL) OXA-10 in complex with VNRX-5133.....	S5
Figure S4. View of the overall fold of the class B metallo- β -lactamase (MBL) NDM-1 in complex with VNRX-5133.....	S6
Figures S5-S31 Analytical data.....	S7-S33
Figure S32. LC-MS spectrum of 13 (VNRX-5133).....	S34
Table S1. Error analysis for the obtained inhibition values.....	S35
Figure S33. Time course evaluation of pIC ₅₀ shifts of VNRX-5133 against subclass B1 MBL NDM-1.....	S36
Table S2. Time-dependent inhibition of subclass B1 MBL NDM-1 by VNRX-5133.....	S36
Table S3. Processing and refinement statistics for NDM-1 / OXA-10 with VNRX-5133	S37
Table S4. Molprobity validation report for OXA-10:VNRX-5133.....	S38
Table S5. Molprobity validation report for NDM-1:VNRX-5133.....	S38
References	S39

Figure S1. Comparison of the binding modes of VNRX-5133 and benzylpenicillin. Overlay of views from VNRX-5133 (PDB ID: 6RTN, yellow) and hydrolysed benzylpenicillin (PDB ID: 2WGI¹, orange) in complex with the Class D serine-β-lactamase OXA-10. The nucleophilic Ser67 residue is in white.

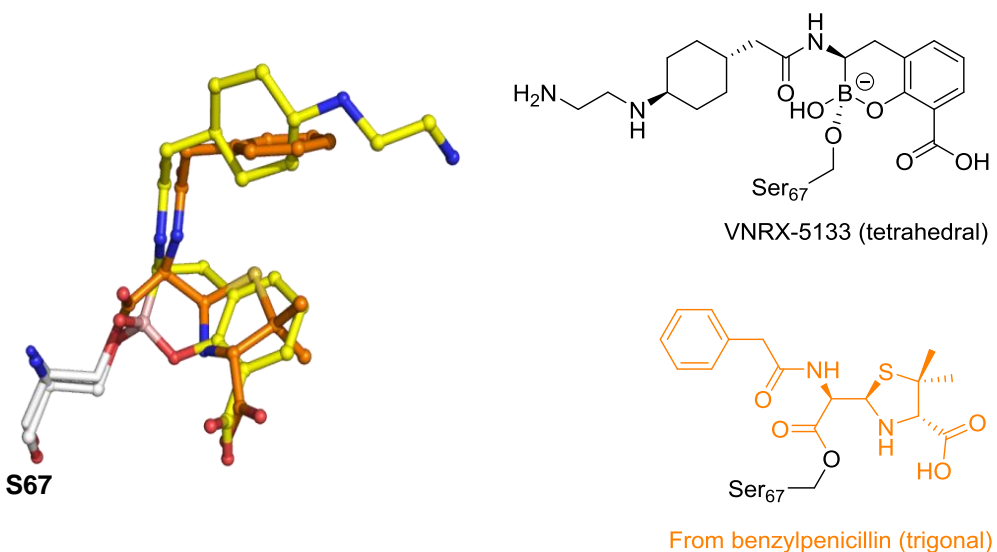
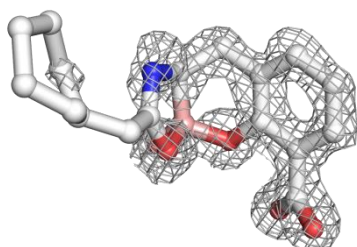


Figure S2. Crystal structure views of the tricyclic forms of VNRX-5133 in complex with NDM-1.

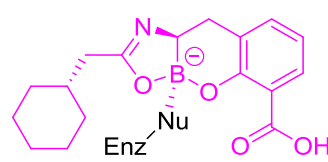
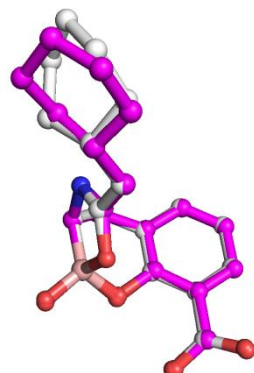
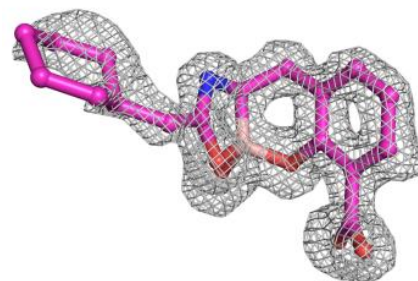
1. (A) Omit 2mFo-DFc electron densities (grey mesh) for the tricyclic inhibitor form in Chain A (white, left) and Chain B (magenta, right) contoured to 2.8σ and 3σ , respectively; Overlay of views of the tricyclic VNRX-5133 forms in chains A and B (in white and magenta, respectively) in the asymmetric unit of NDM-1 (PDB ID: 6RFM); **(B)** Comparison of the binding modes of the tricyclic forms of VNRX-5133 and hydrolysed benzylpenicillin (PDB ID: 4EYF², green). Notably, zinc ions (spheres) are positioned similarly in both structures.

A

Tricyclic inhibitor form, Chain A:



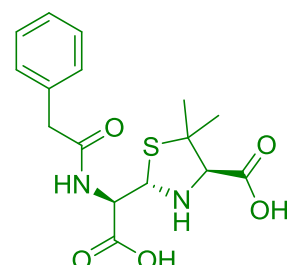
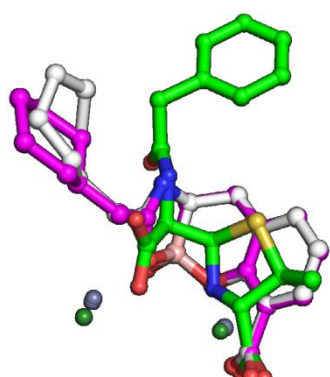
Tricyclic inhibitor form, Chain B:



VNRX-5133
(tricyclic sp^3 form)

Enz-Nu = Enz-(Zn^{II})_n-OH

B



hydrolyzed benzylpenicillin

+ Enz-Nu = Enz-(Zn^{II})_n-OH

Figure S3. View of the overall fold of the class D serine- β -lactamase (SBL) OXA-10 in complex with VNRX-5133. Cartoon representation containing both molecules in the asymmetric unit (grey, chains A and B, PDB 6RTN). The ligand (VNRX-5133, yellow) bound as a bicyclic tetrahedral complex and the carbamylated Lys70 residue (KCX, orange) are shown as sticks. The α -helices containing the nucleophilic serine residue are in cyan, and the conserved Ω -loop common to Class A SBLs and penicillin-binding proteins are in red.

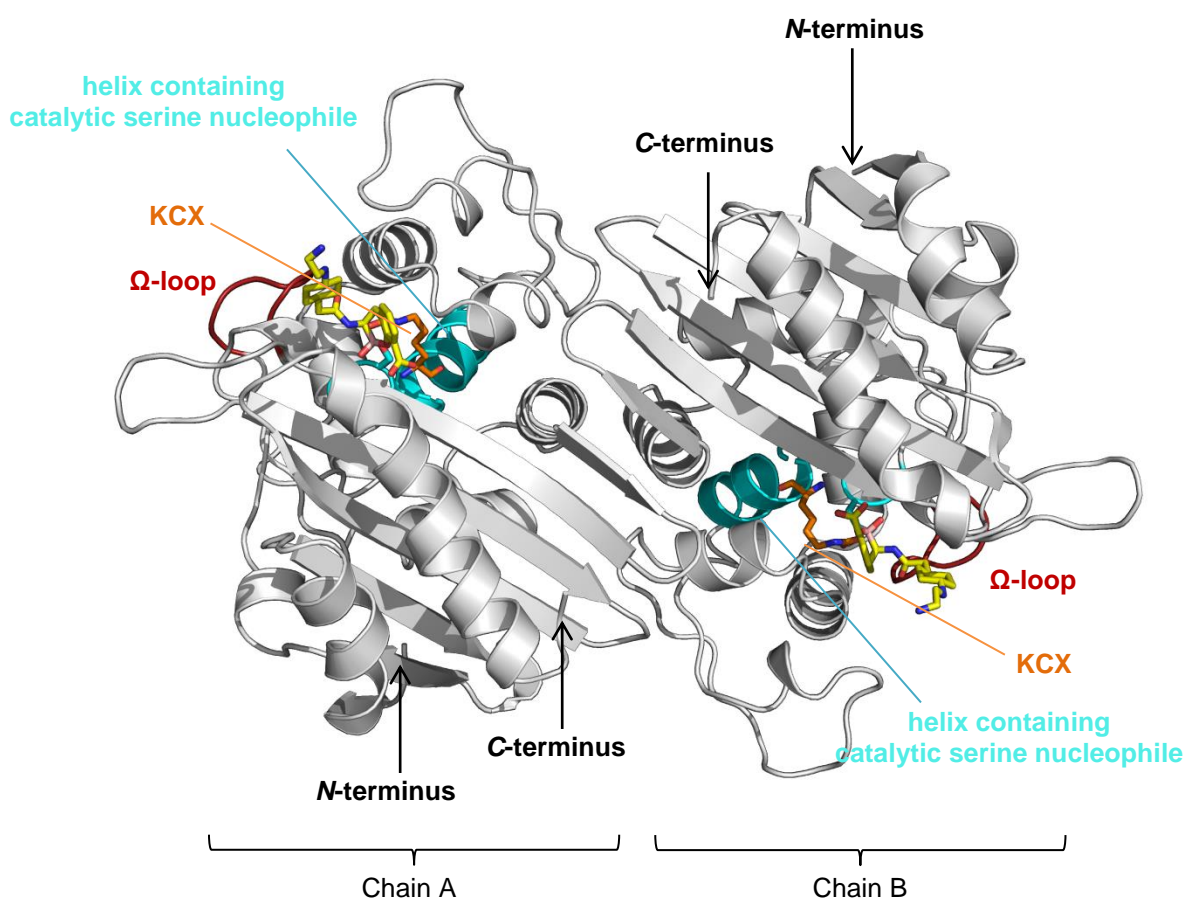
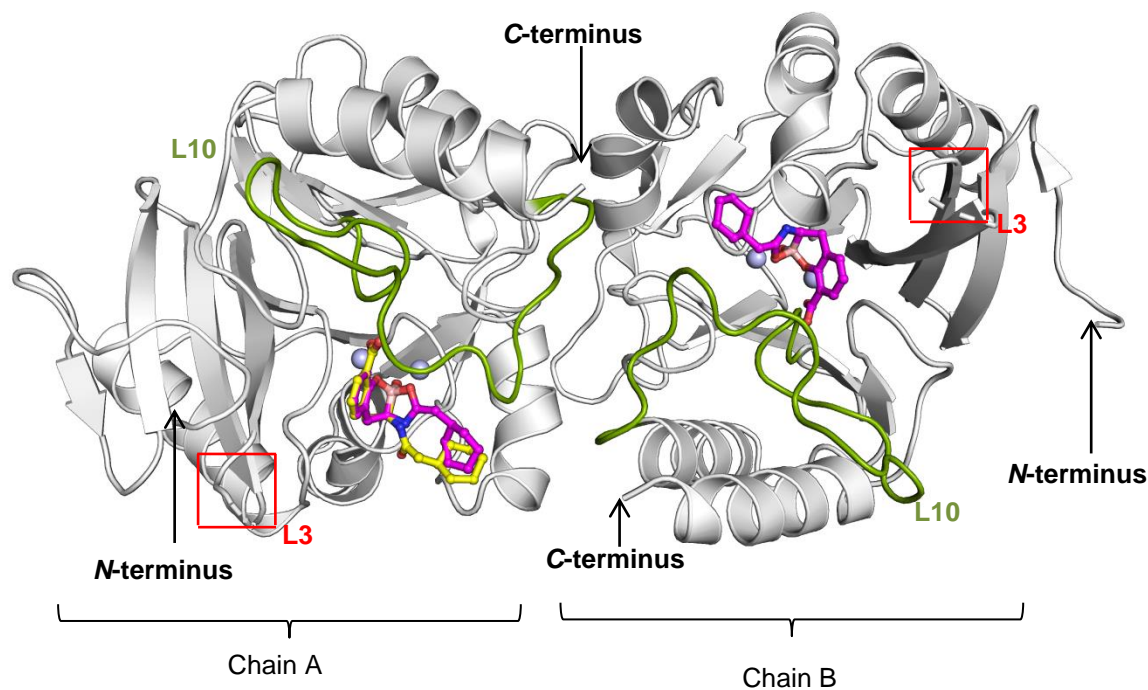


Figure S4. View of the overall fold of the class B metallo- β -lactamase (MBL) NDM-1 in complex with VNRX-5133. Cartoon representation showing both protein molecules in the asymmetric unit (grey, chains A and B, PDB ID: 6RFM). The ligand (VNRX-5133) observed in either bicyclic (yellow) or tricyclic (magenta) tetrahedral forms is shown in ball and stick representation. Zinc ions are shown as purple spheres. The two keys active site loops likely closely involved in the substrate binding and subsequent catalysis are shown: disordered L3 loop areas are marked with red squares; L10 loop is in green.



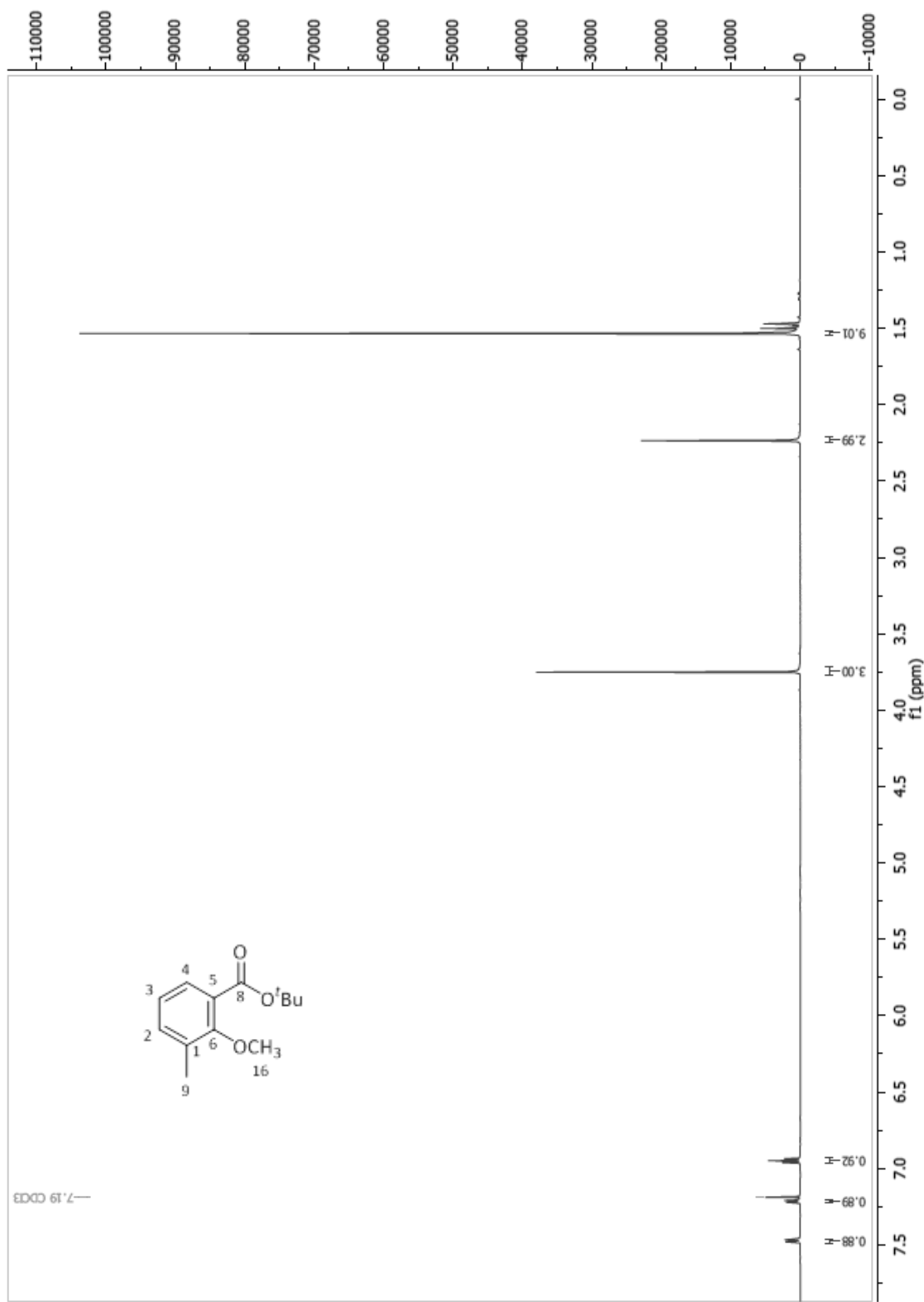


Figure S5. ¹H NMR spectrum of 2.



Figure S6. ^{13}C NMR spectrum of 2.

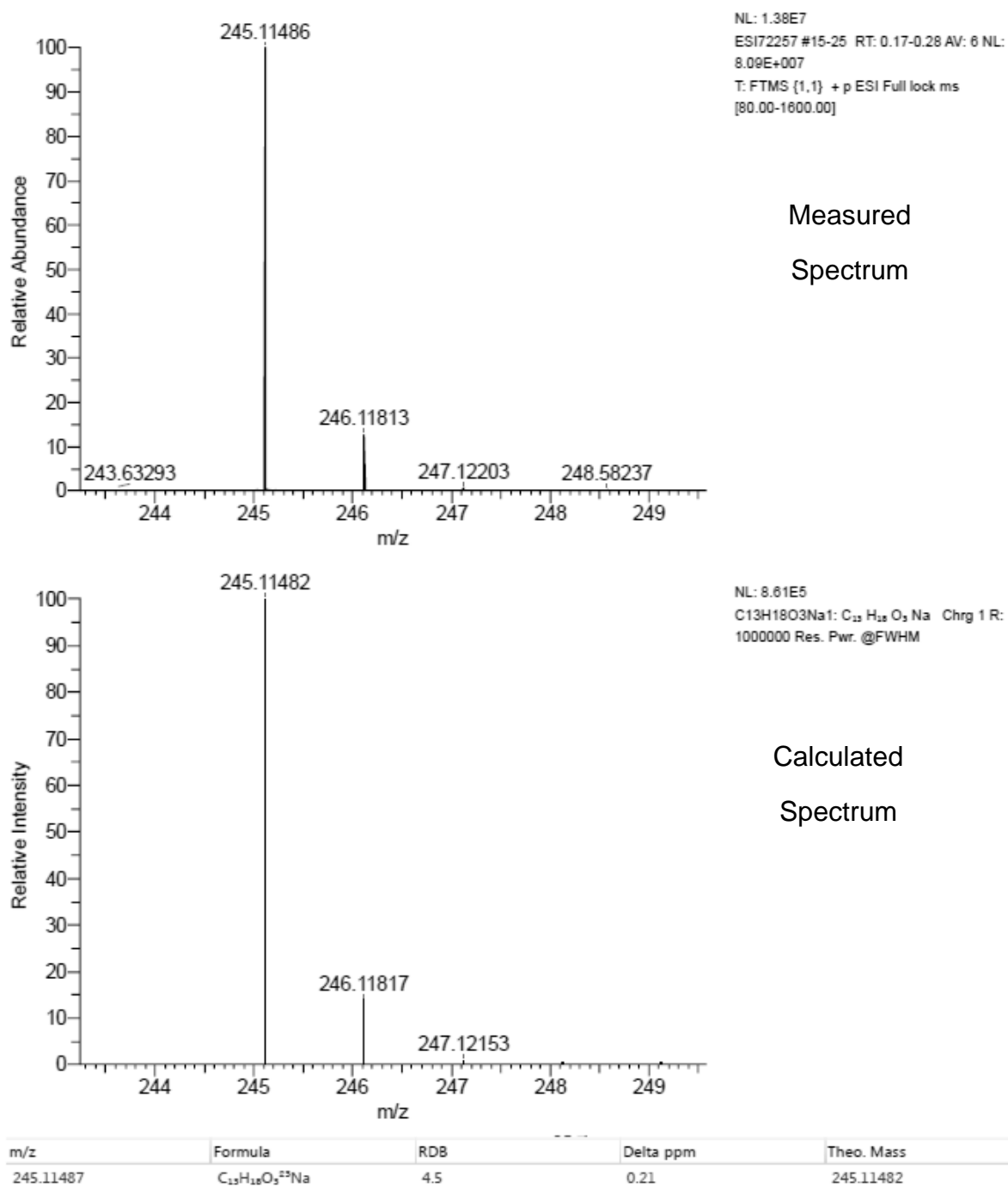


Figure S7. HRMS spectrum of 2.

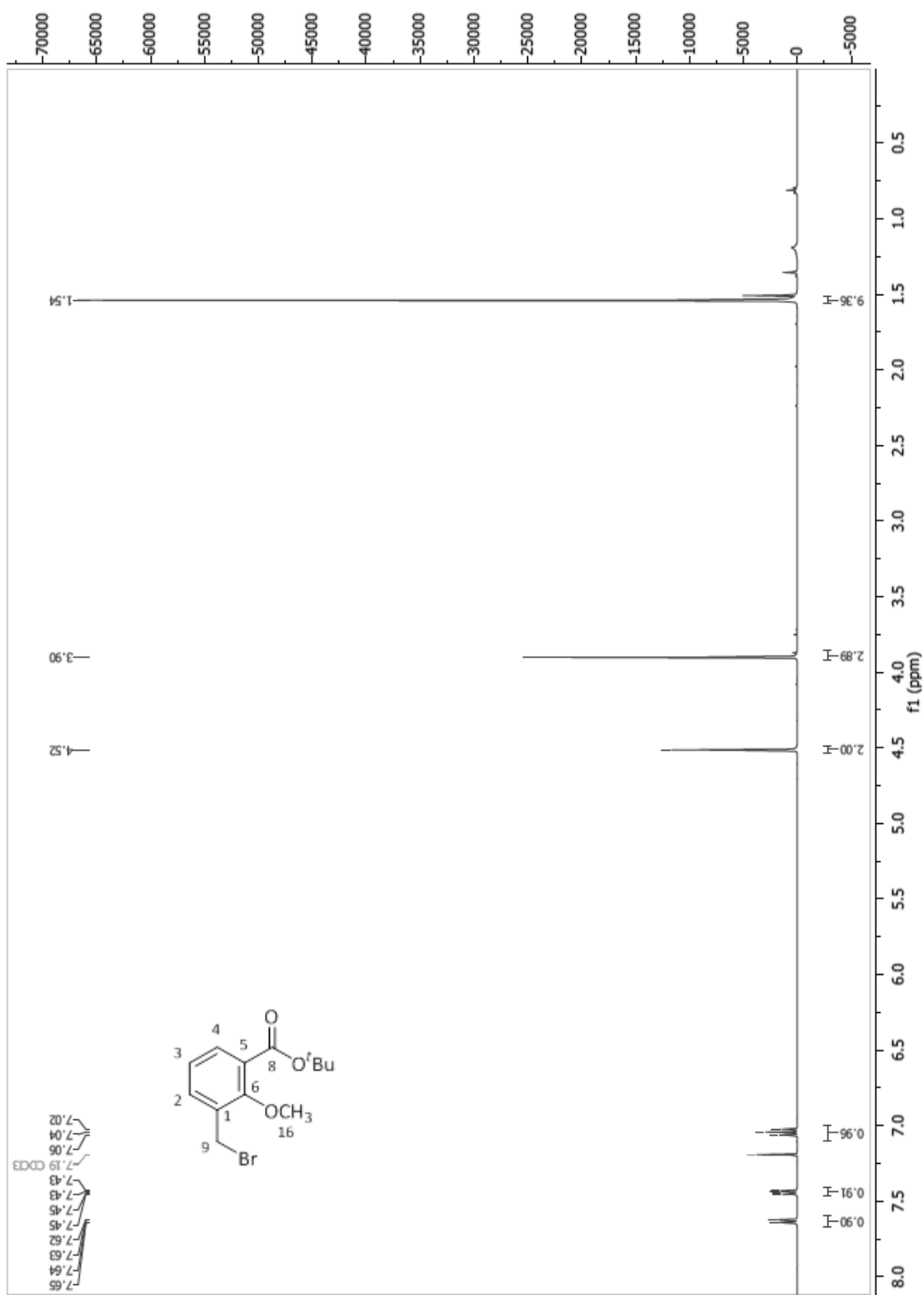


Figure S8. ¹H NMR spectrum of 3.

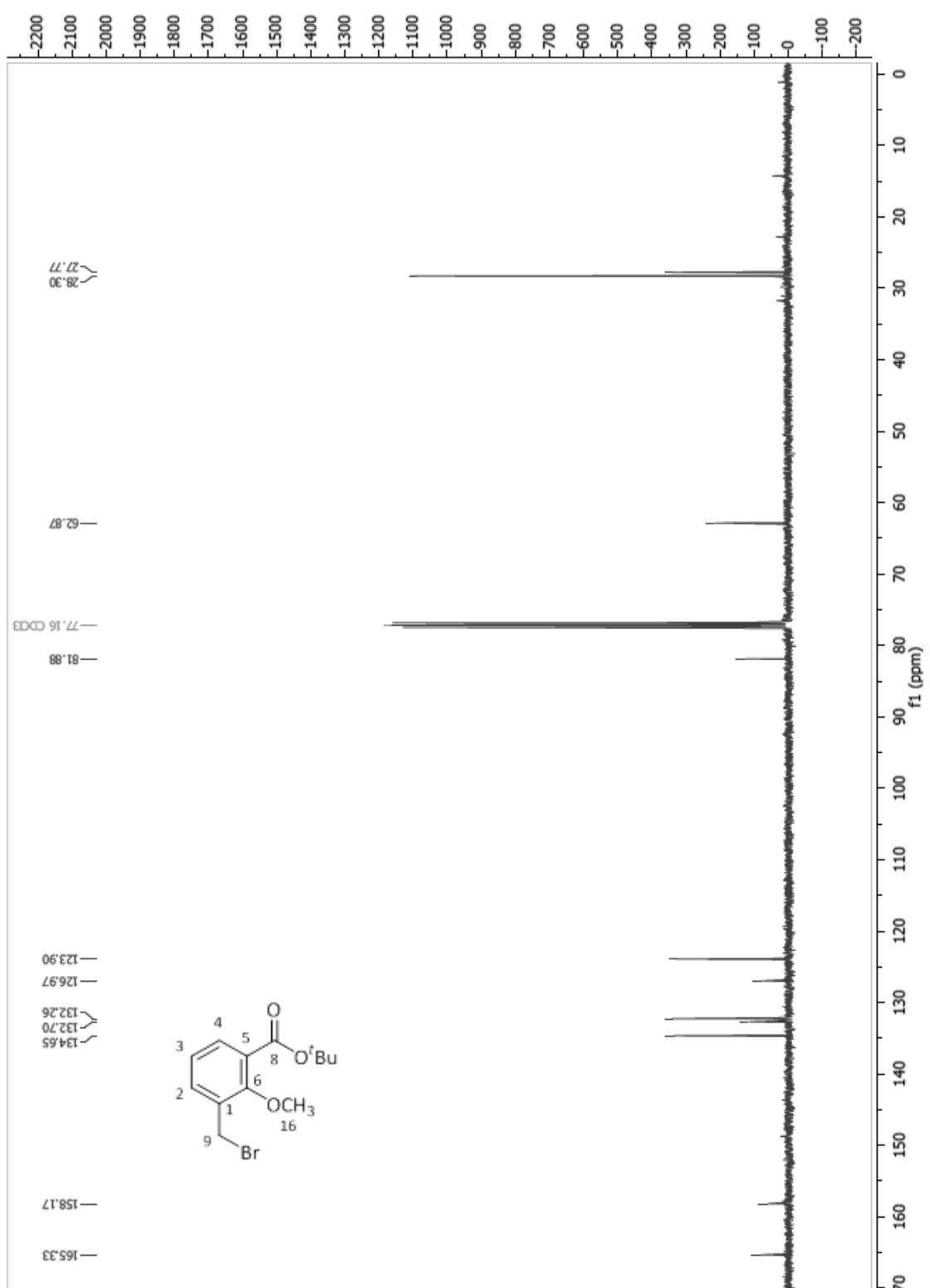


Figure S9. ^{13}C NMR spectrum of 3.

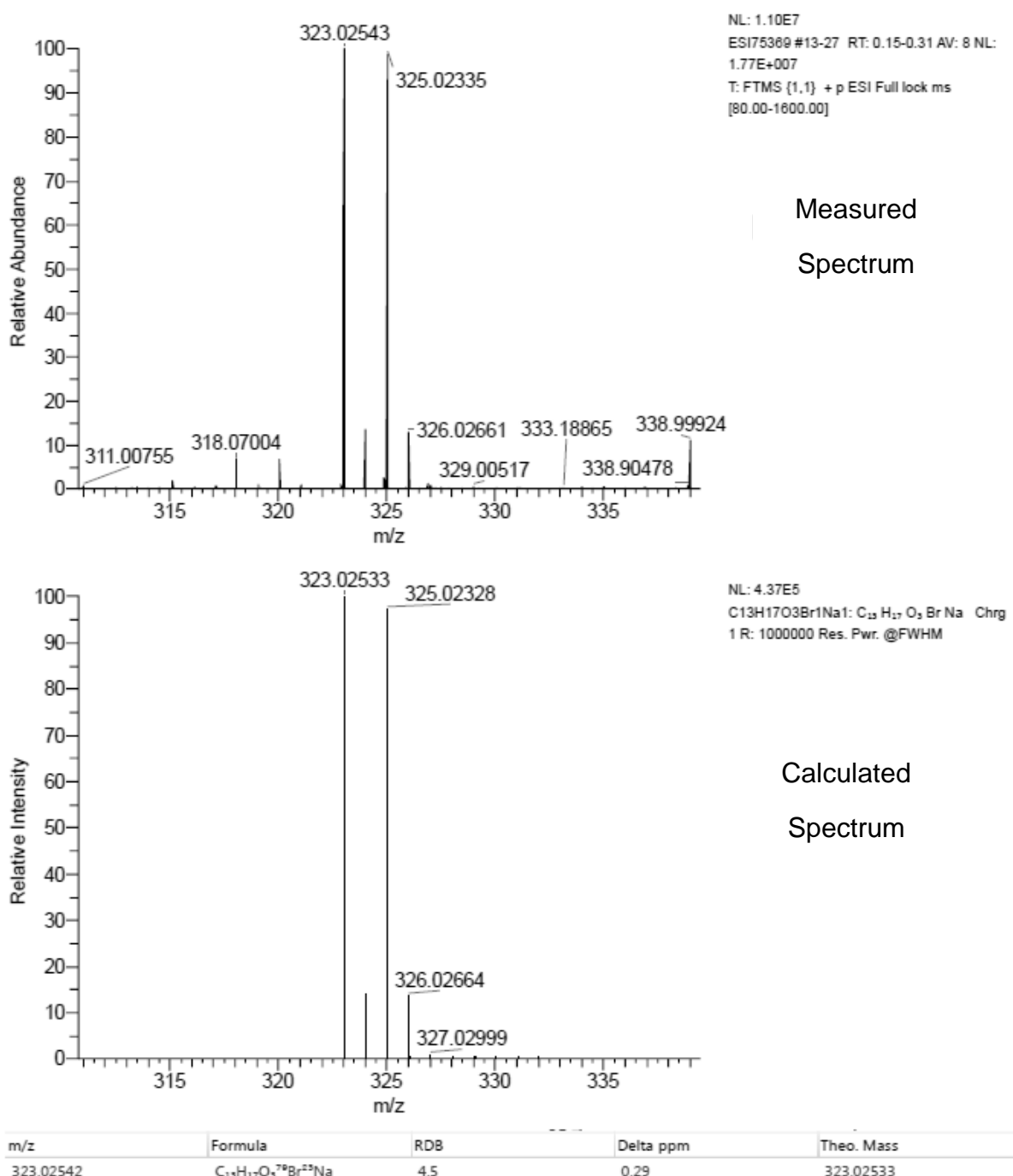


Figure S10. HRMS spectrum of 3.

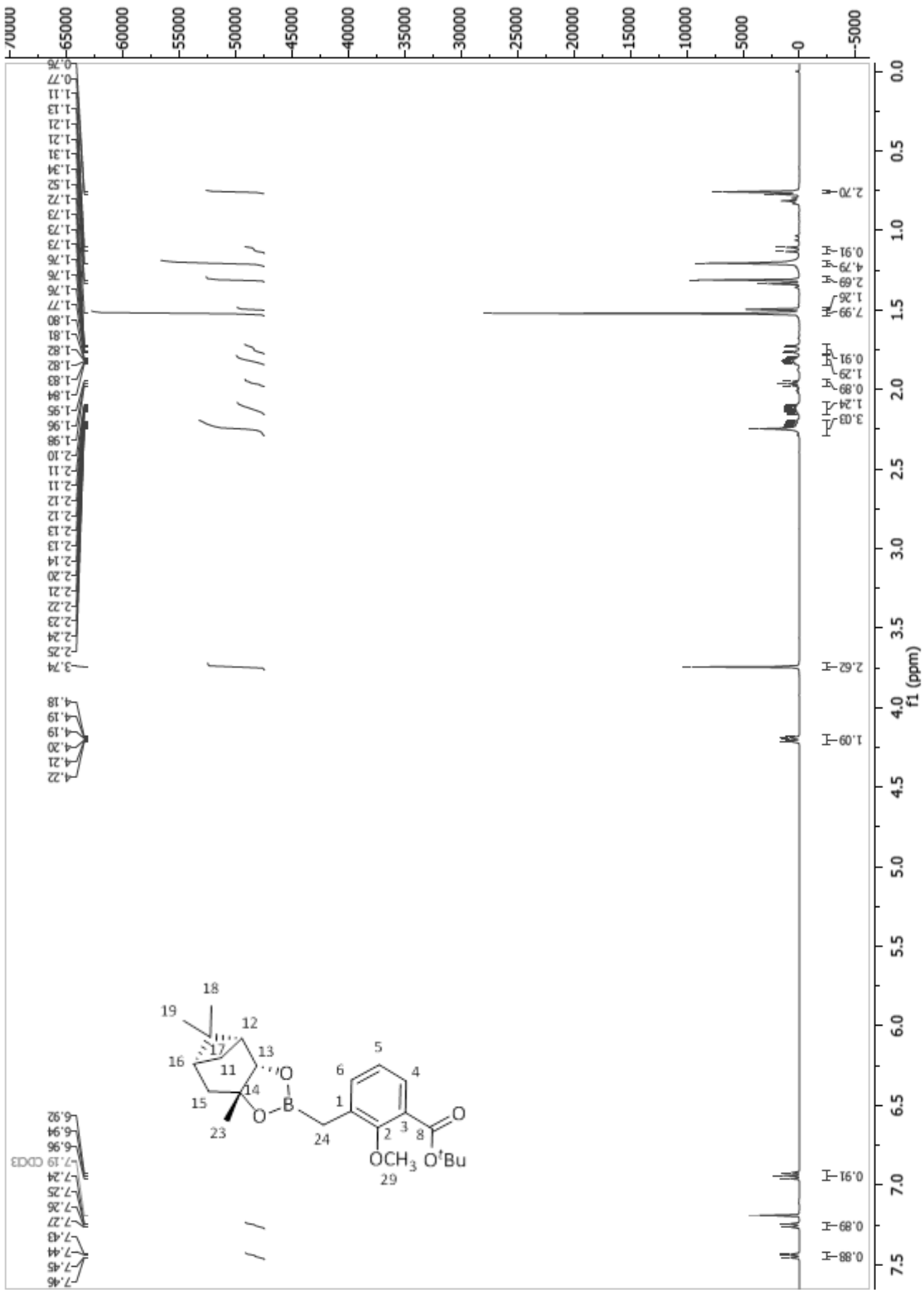


Figure S11. ¹H NMR spectrum of 4.

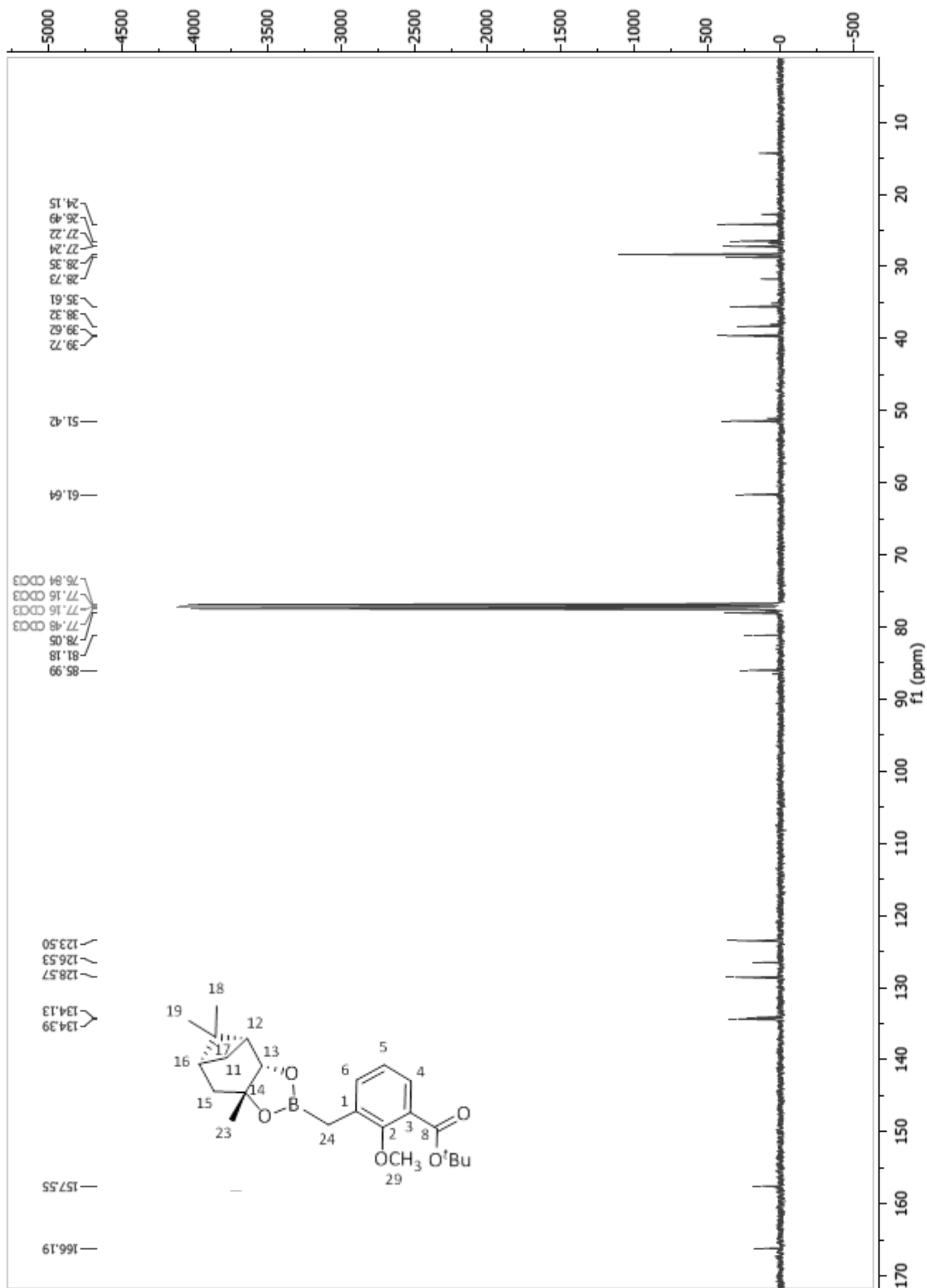


Figure S12. ^{13}C NMR spectrum of 4.

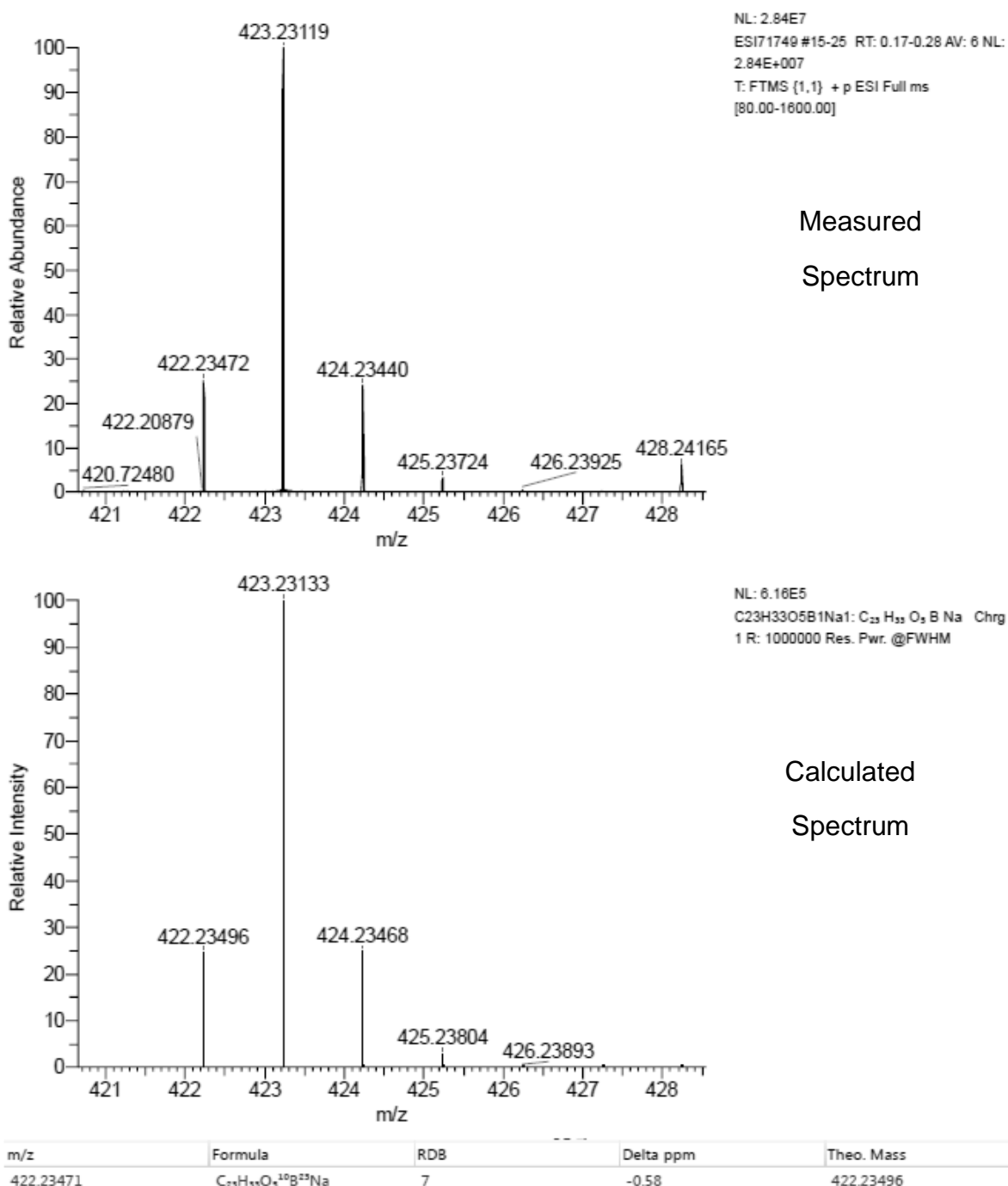


Figure S13. HRMS spectrum of 4.

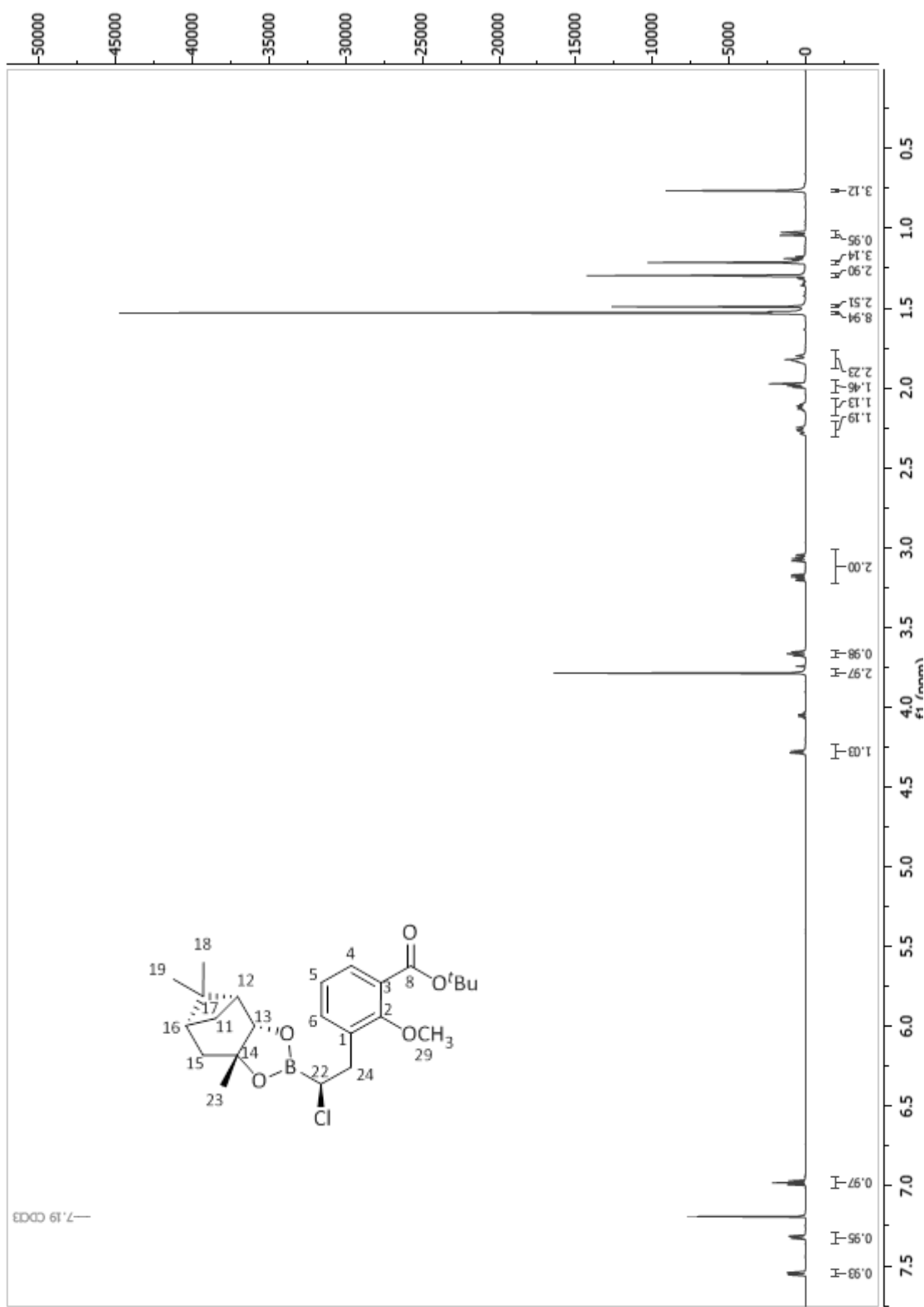


Figure S14. ^1H NMR spectrum of 5.

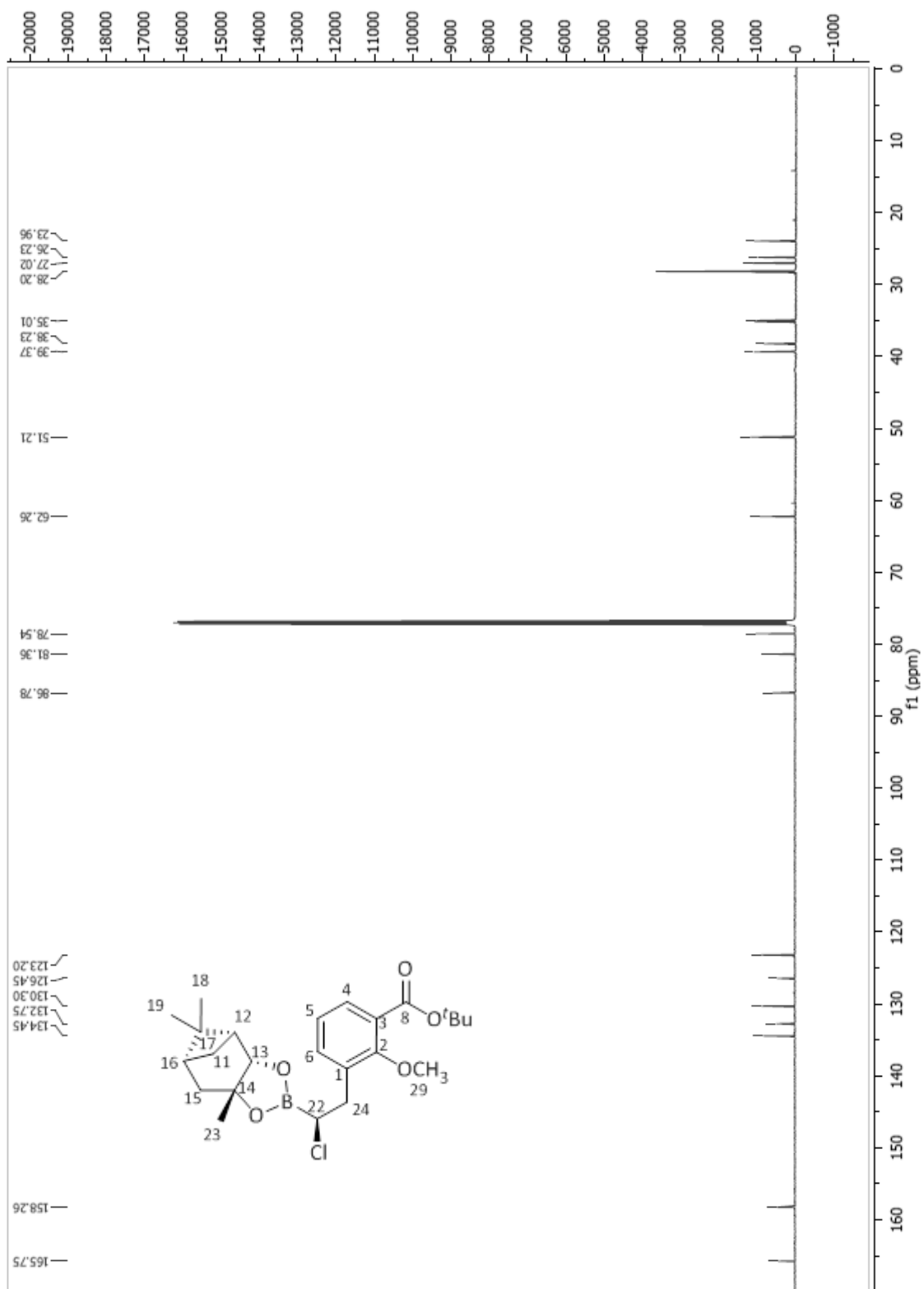


Figure S15. ^{13}C NMR spectrum of 5.

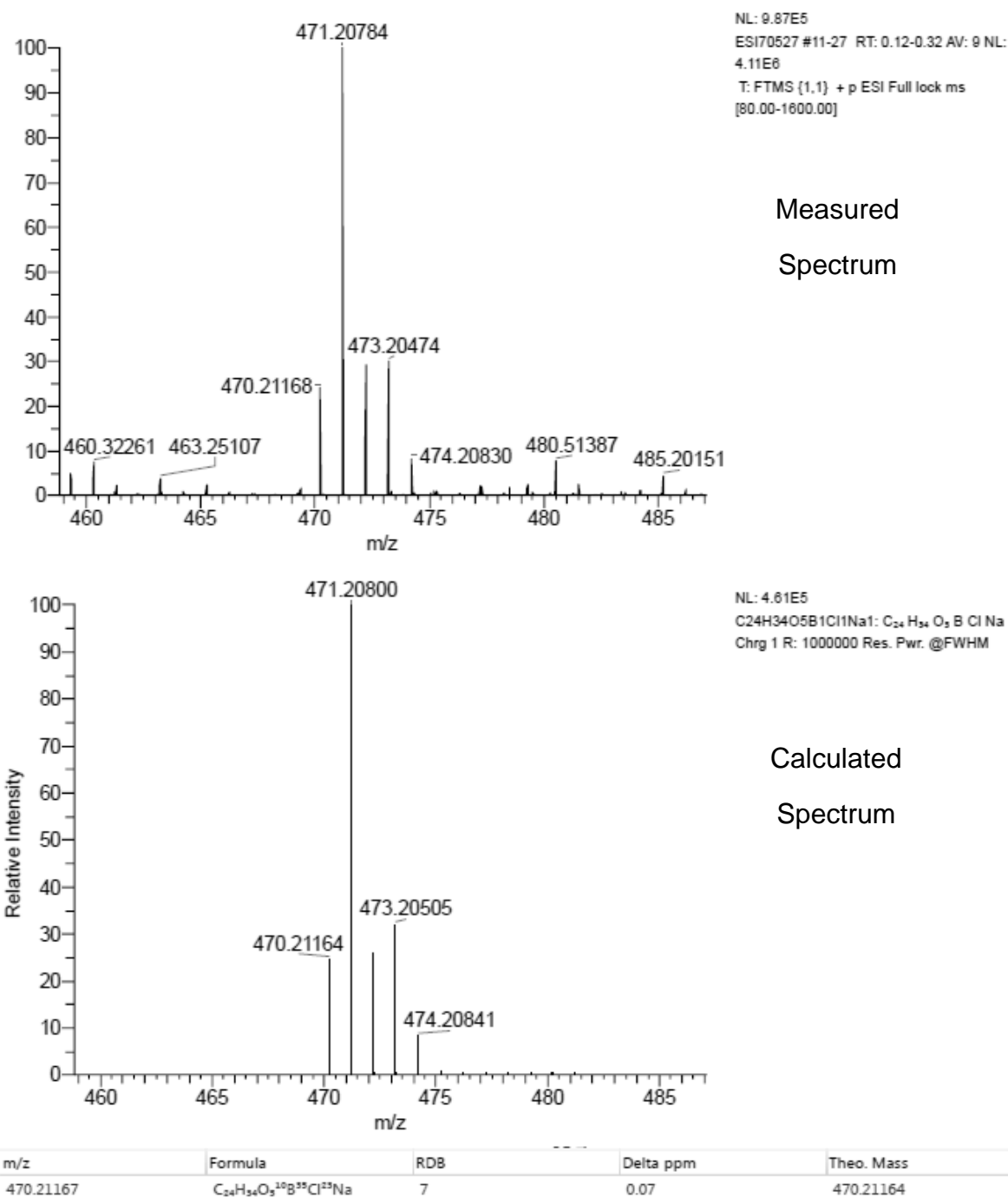


Figure S16. HRMS spectrum of 5.

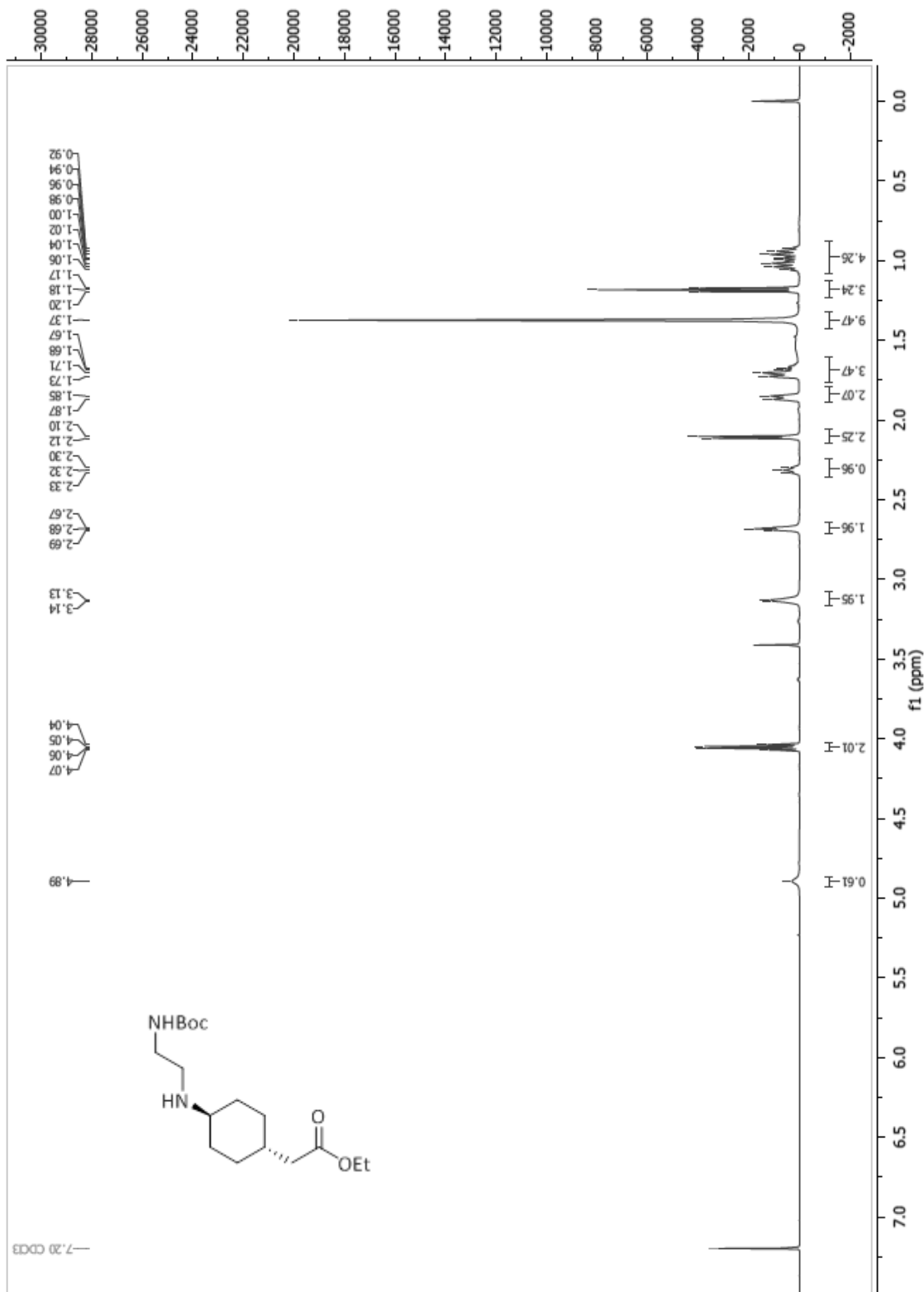


Figure S17. ^1H NMR spectrum of 9.

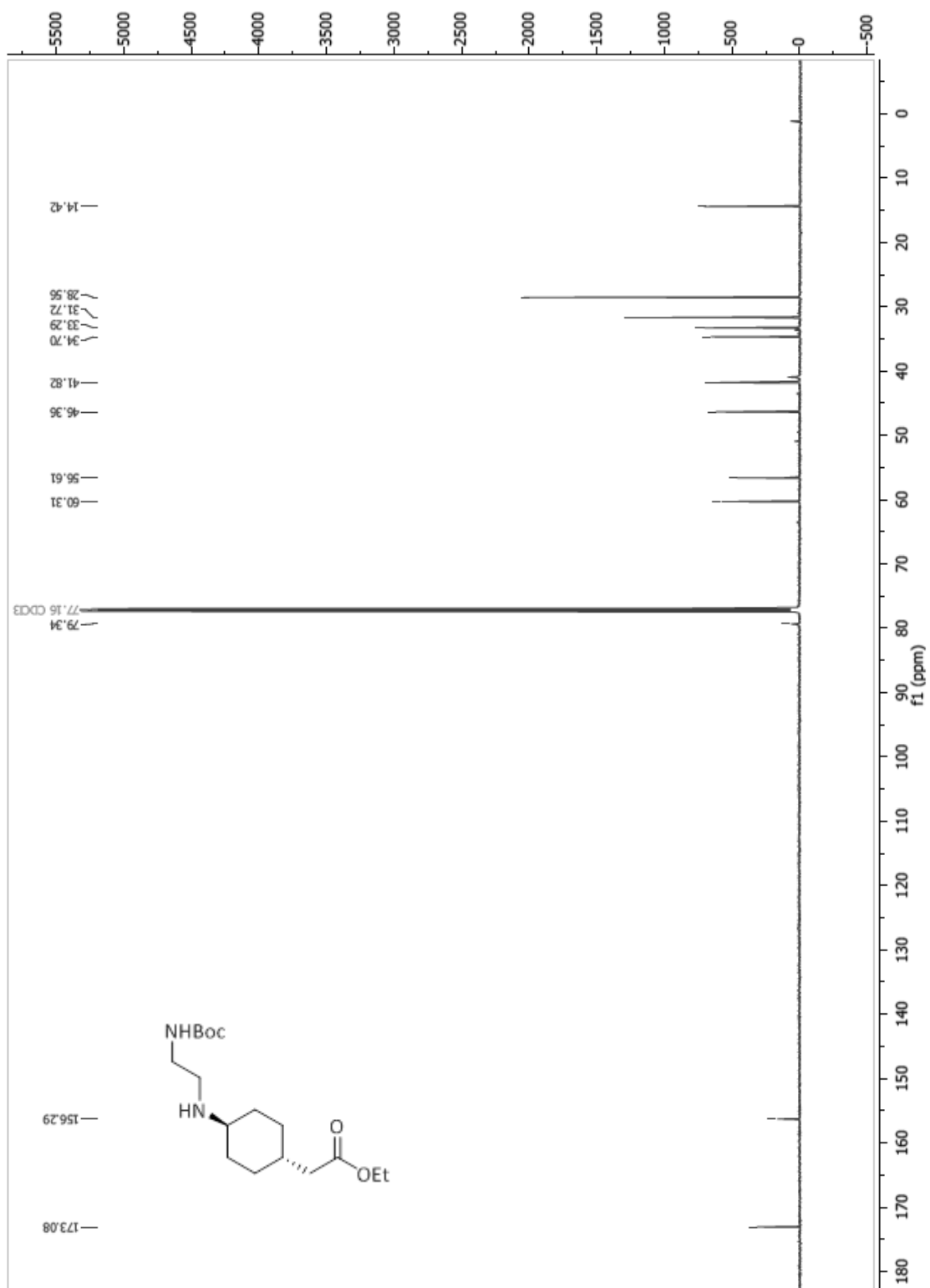


Figure S18. ^{13}C NMR spectrum of 9.

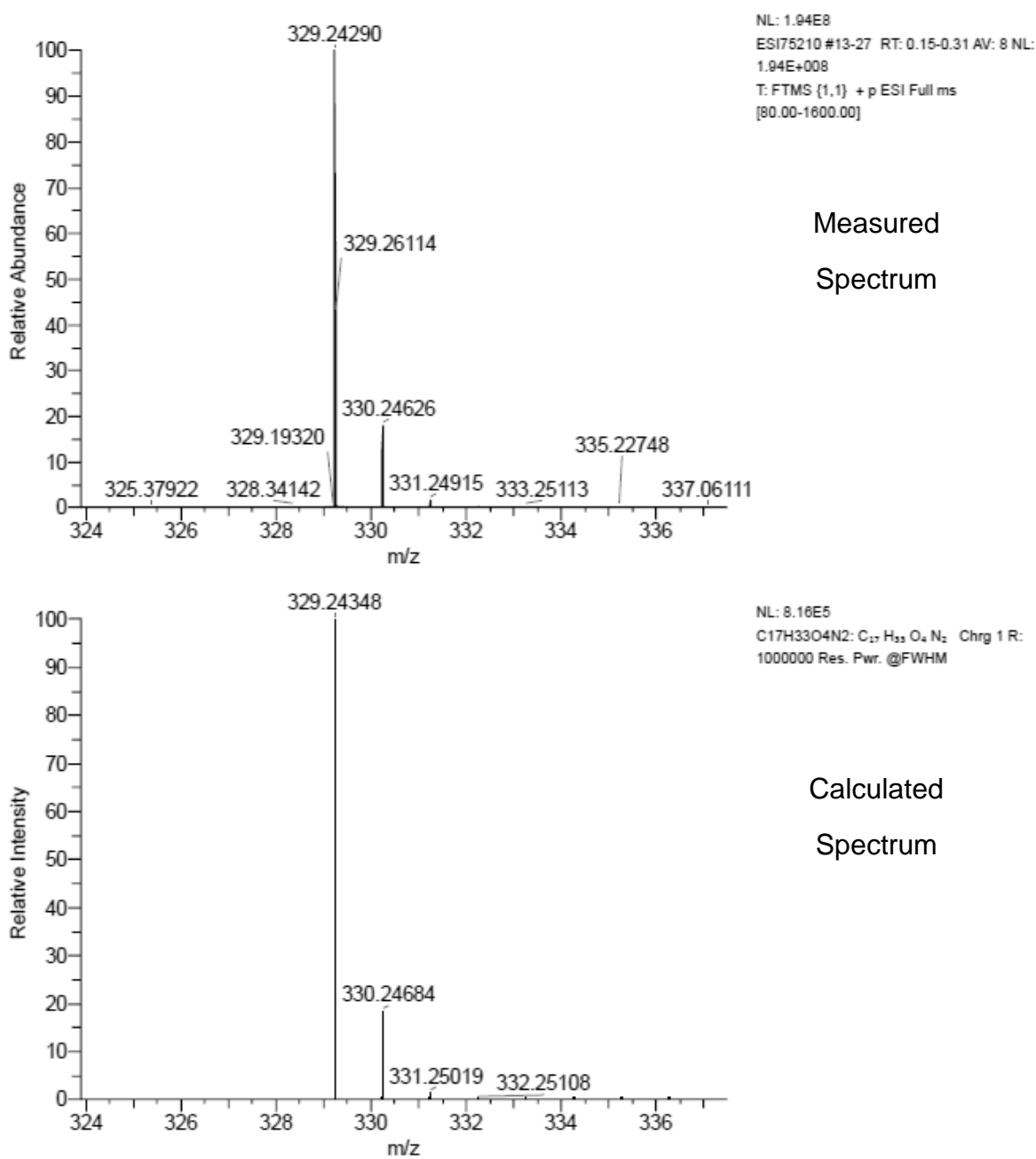


Figure S19. HRMS spectrum of 9.

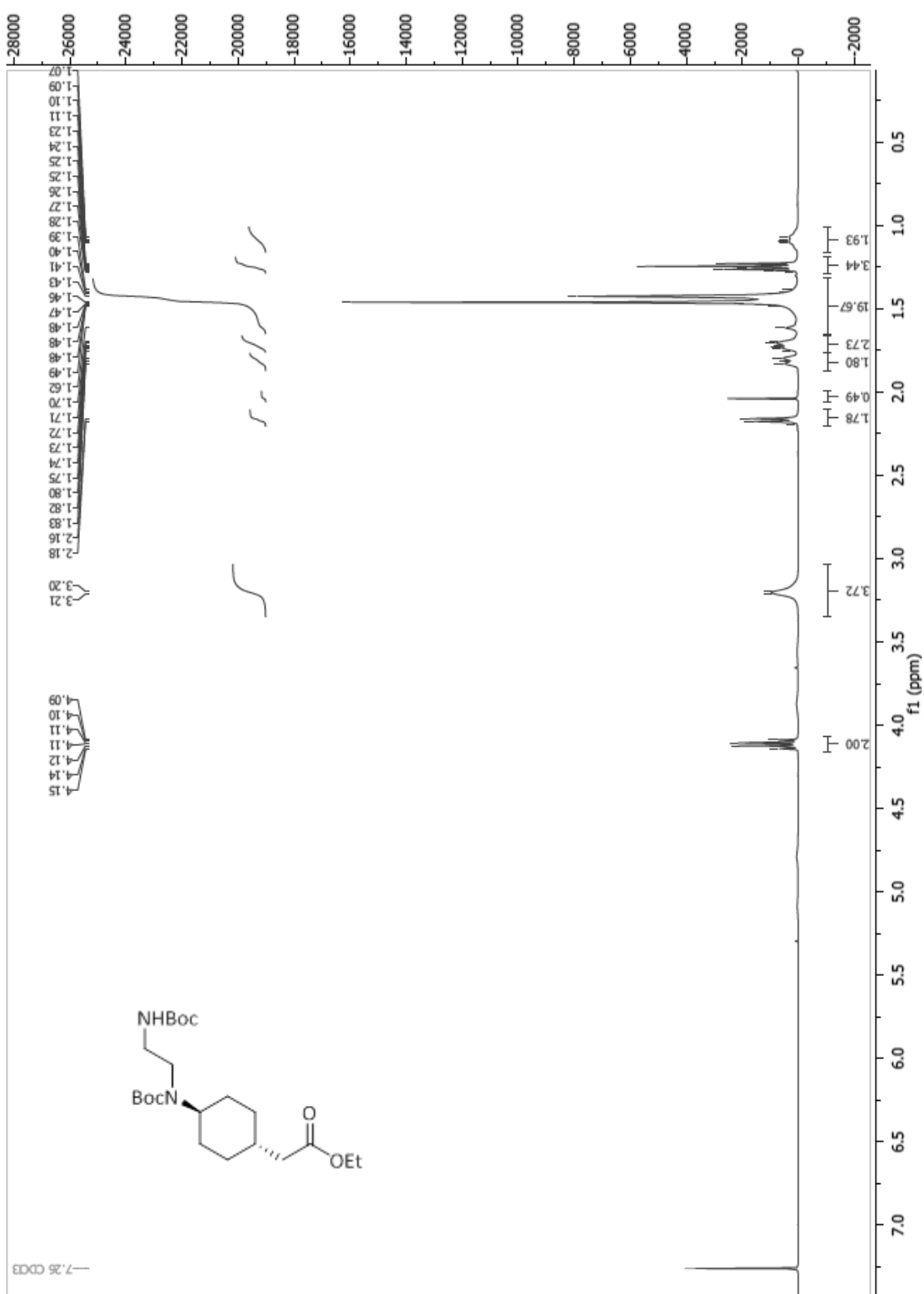


Figure S20. ^1H NMR spectrum of 10.

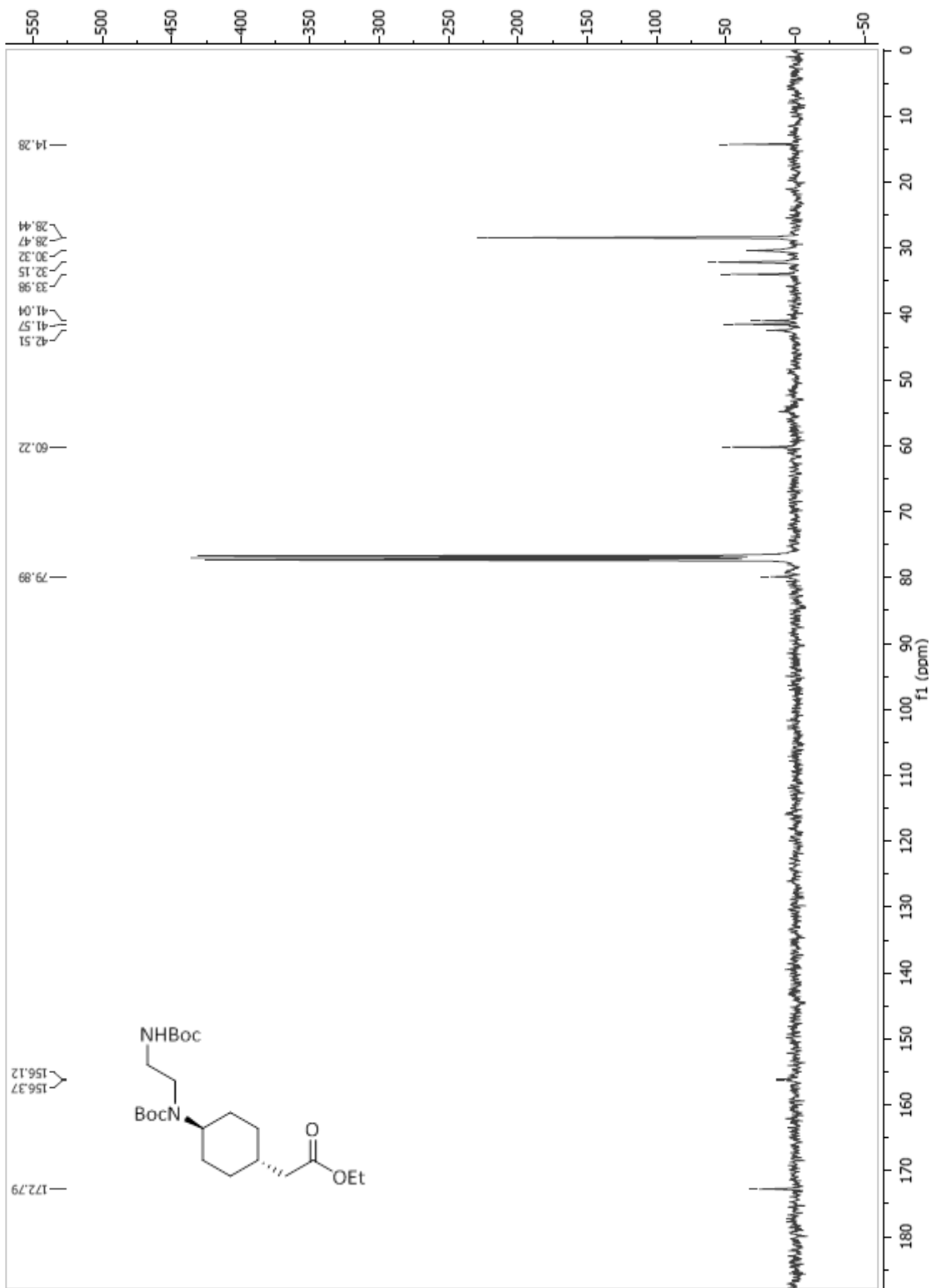


Figure S21. ^{13}C NMR spectrum of 10.

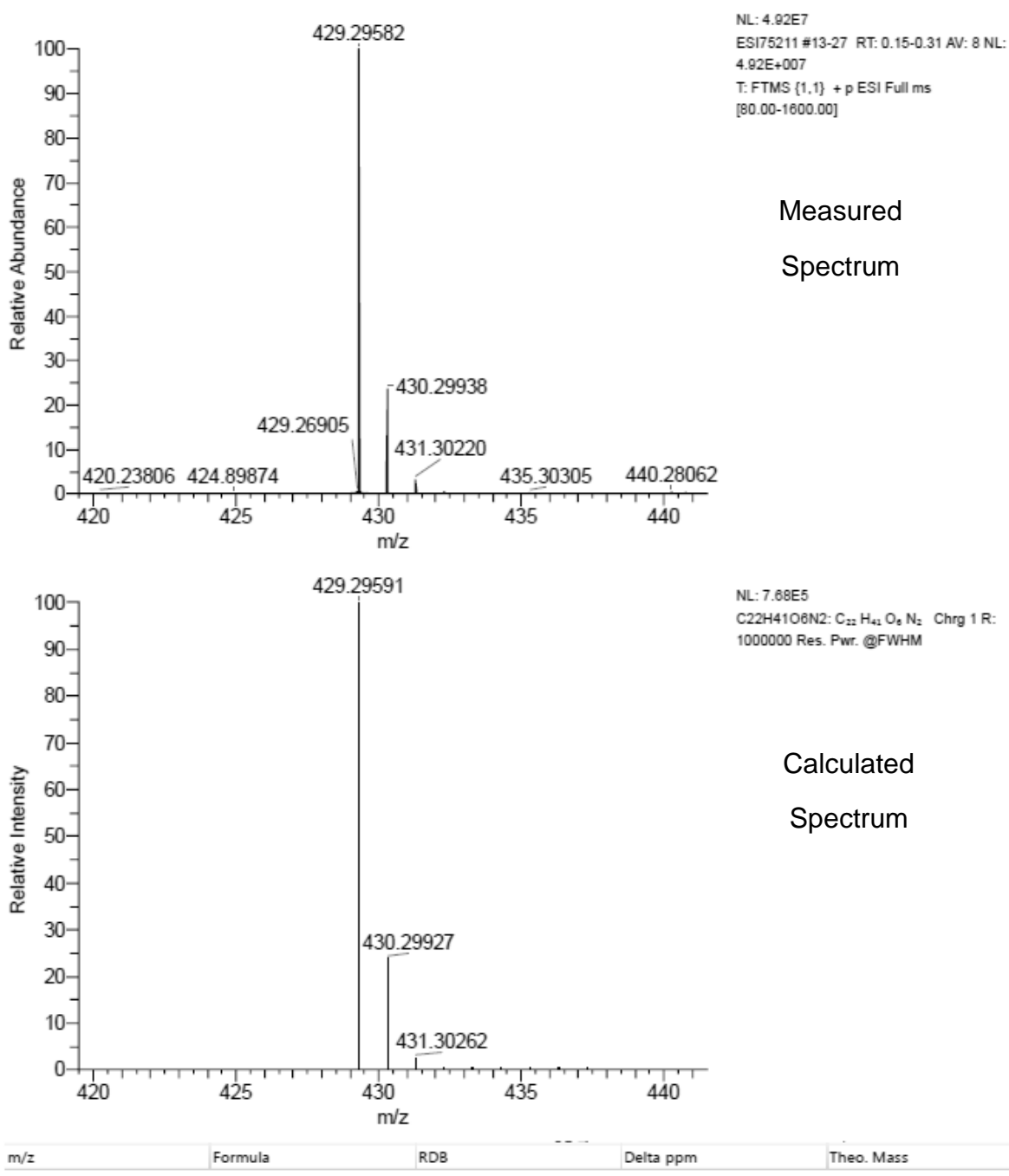


Figure S22. HRMS spectrum of 10.

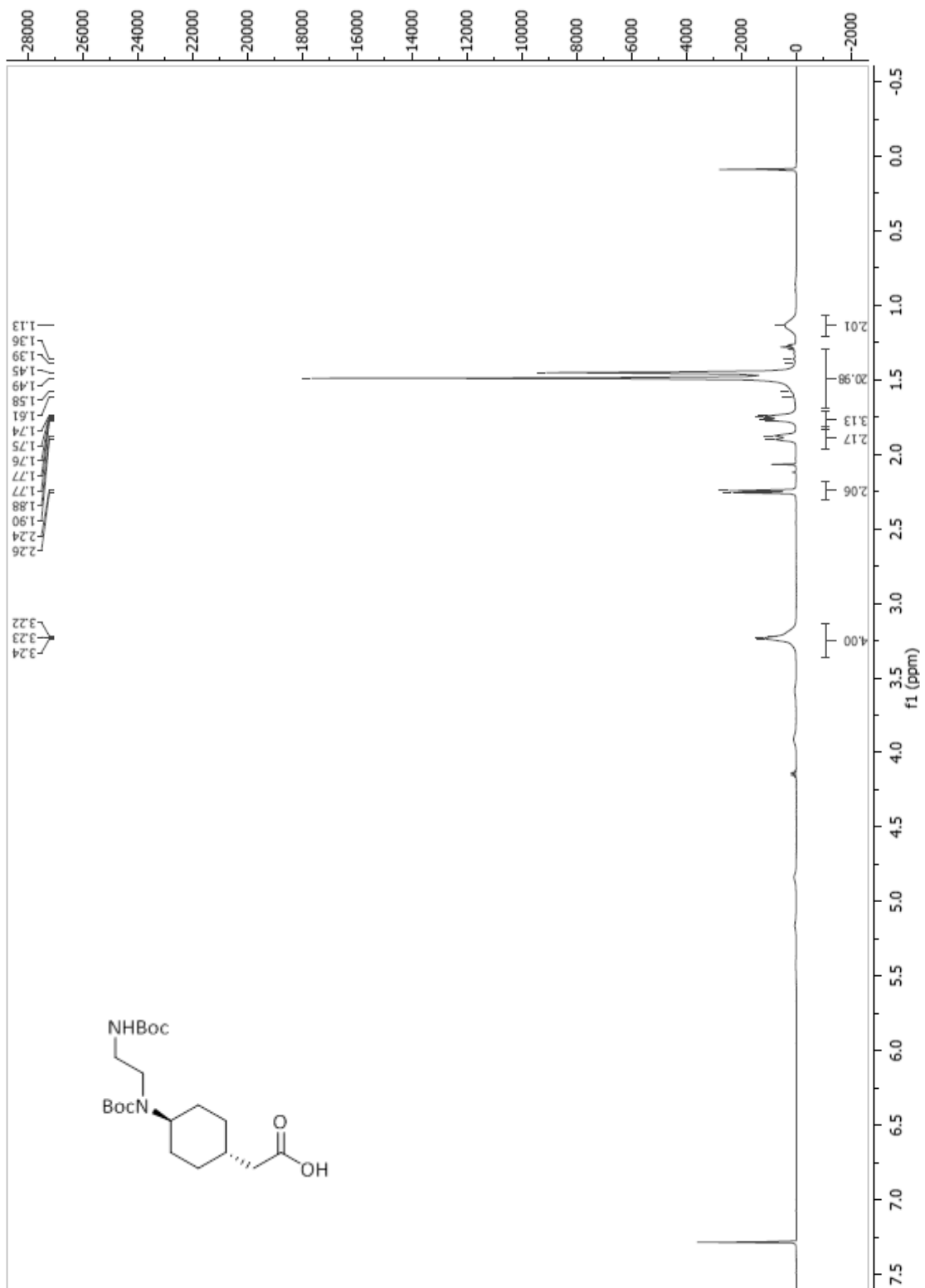


Figure S23. ^1H NMR spectrum of 11.

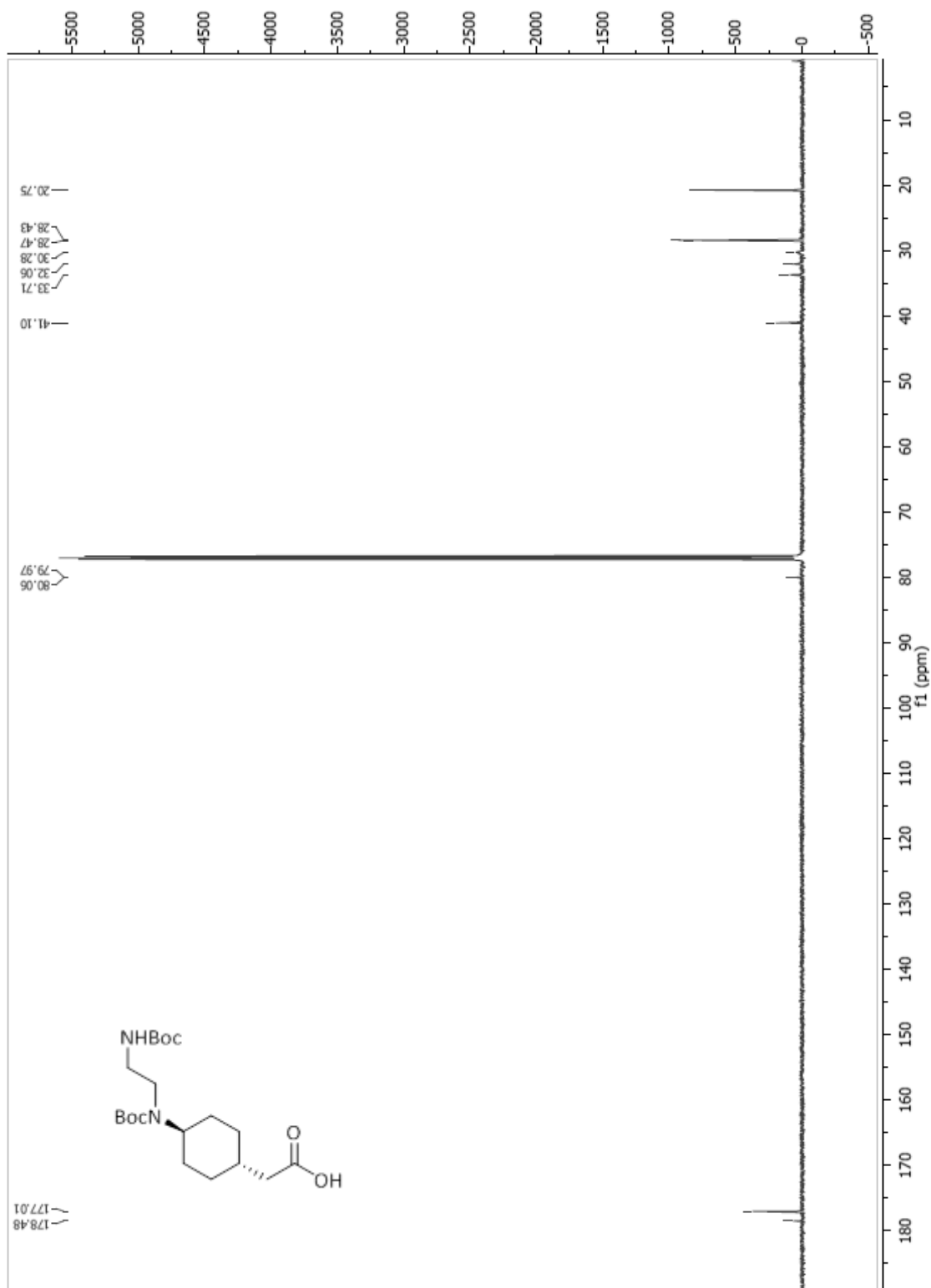


Figure S24. ^{13}C NMR spectrum of 11.

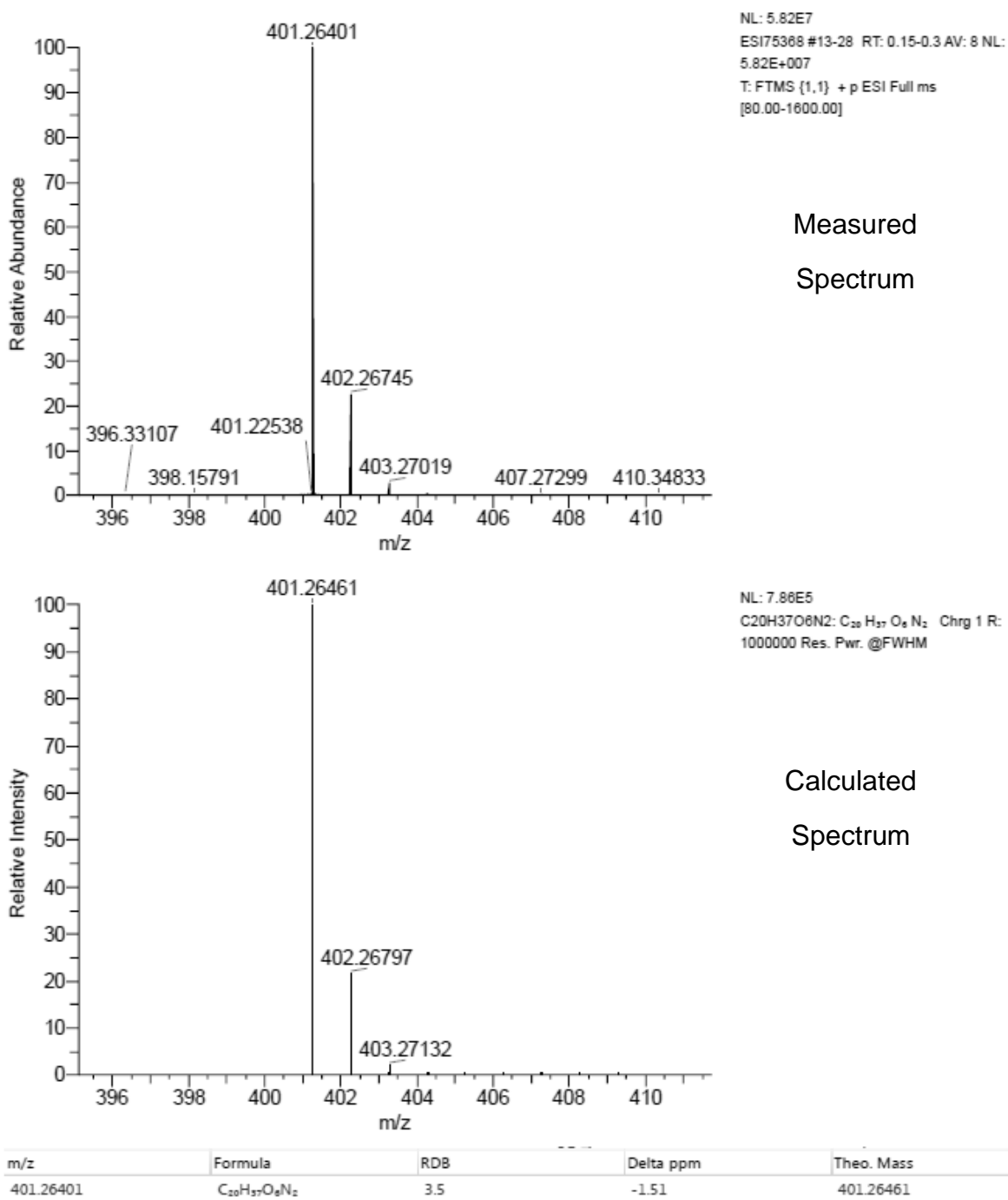
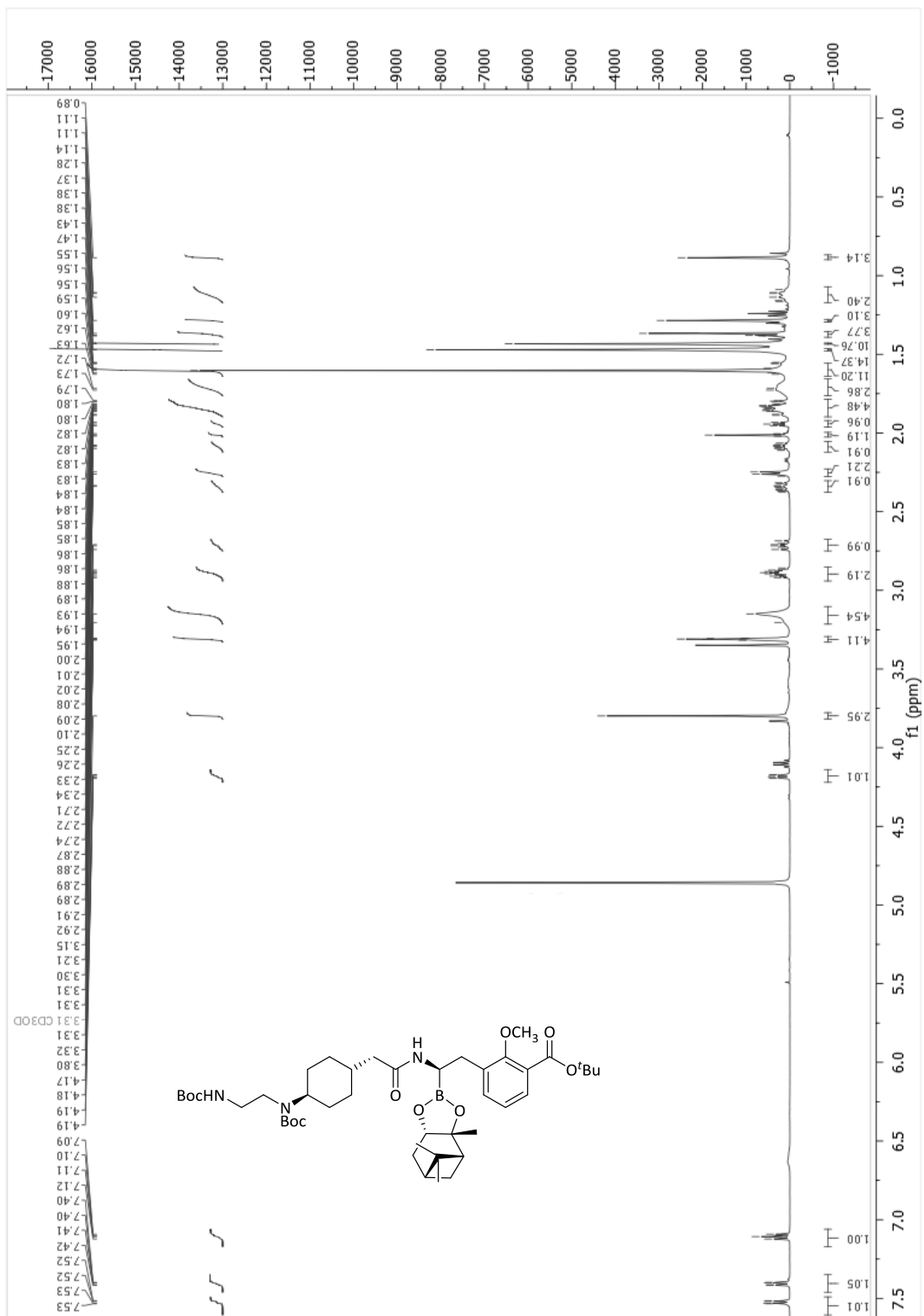


Figure S25. HRMS spectrum of 11.



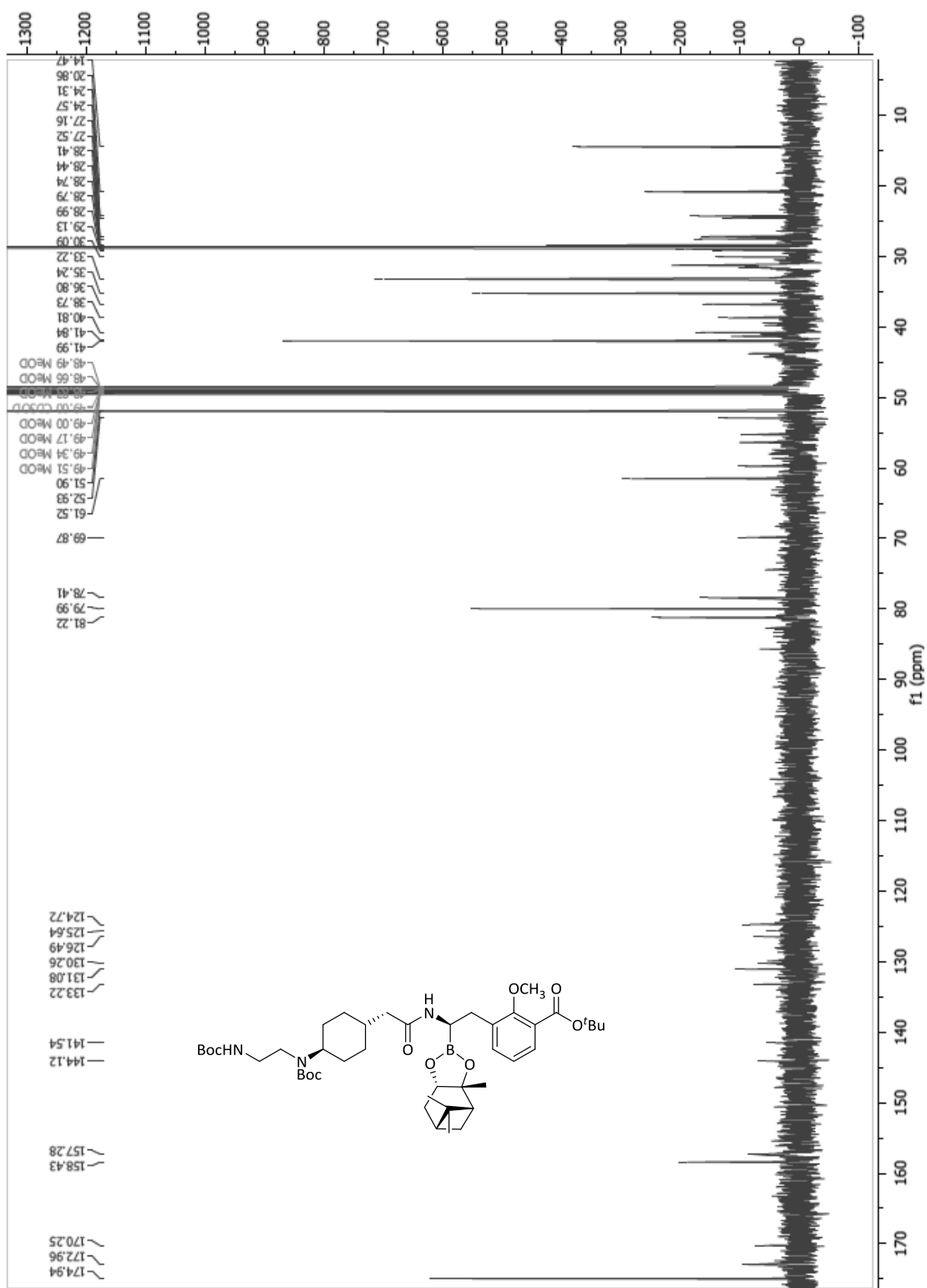


Figure S27. ^{13}C NMR spectrum of 12.

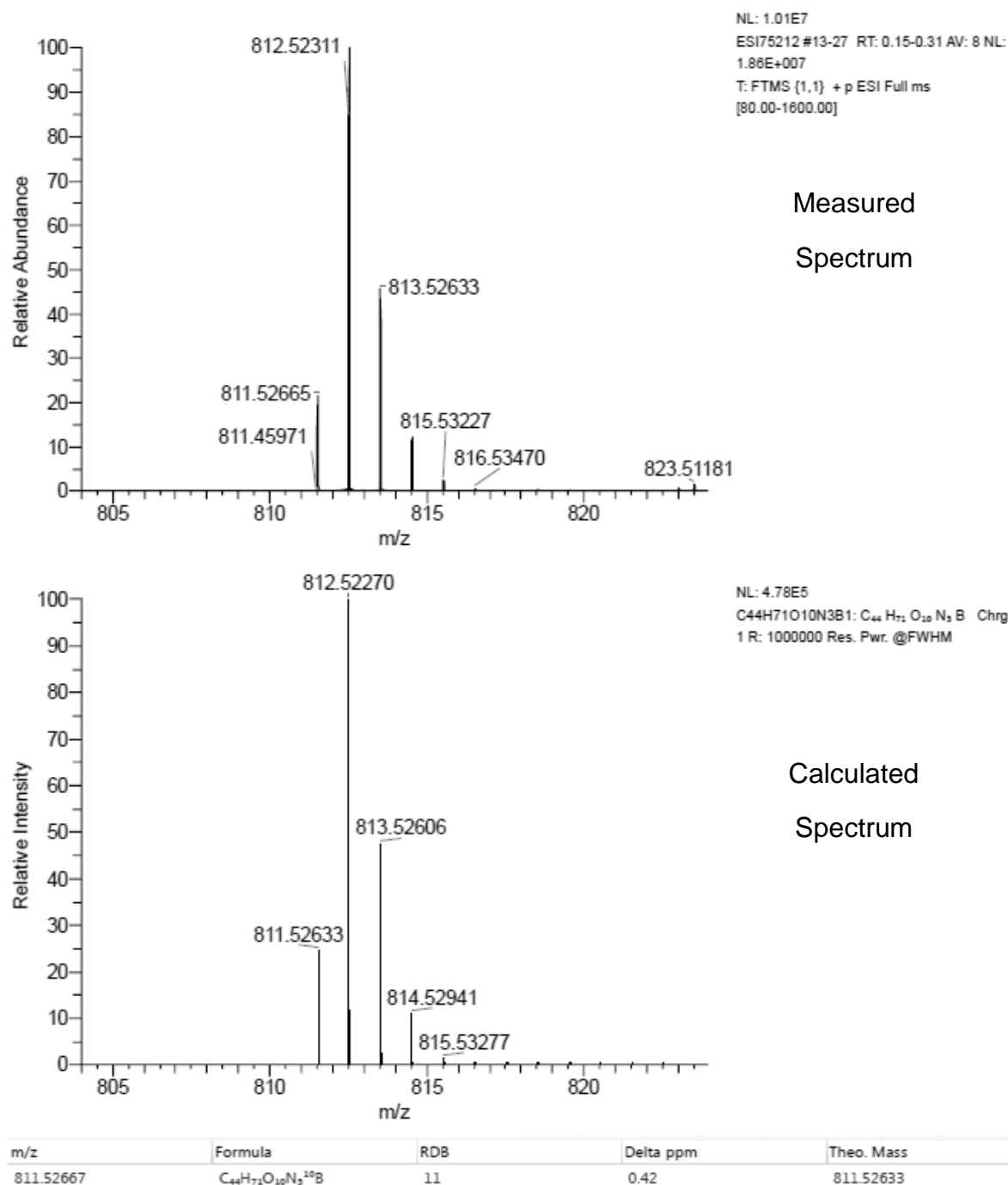


Figure S28. HRMS spectrum of **12**.

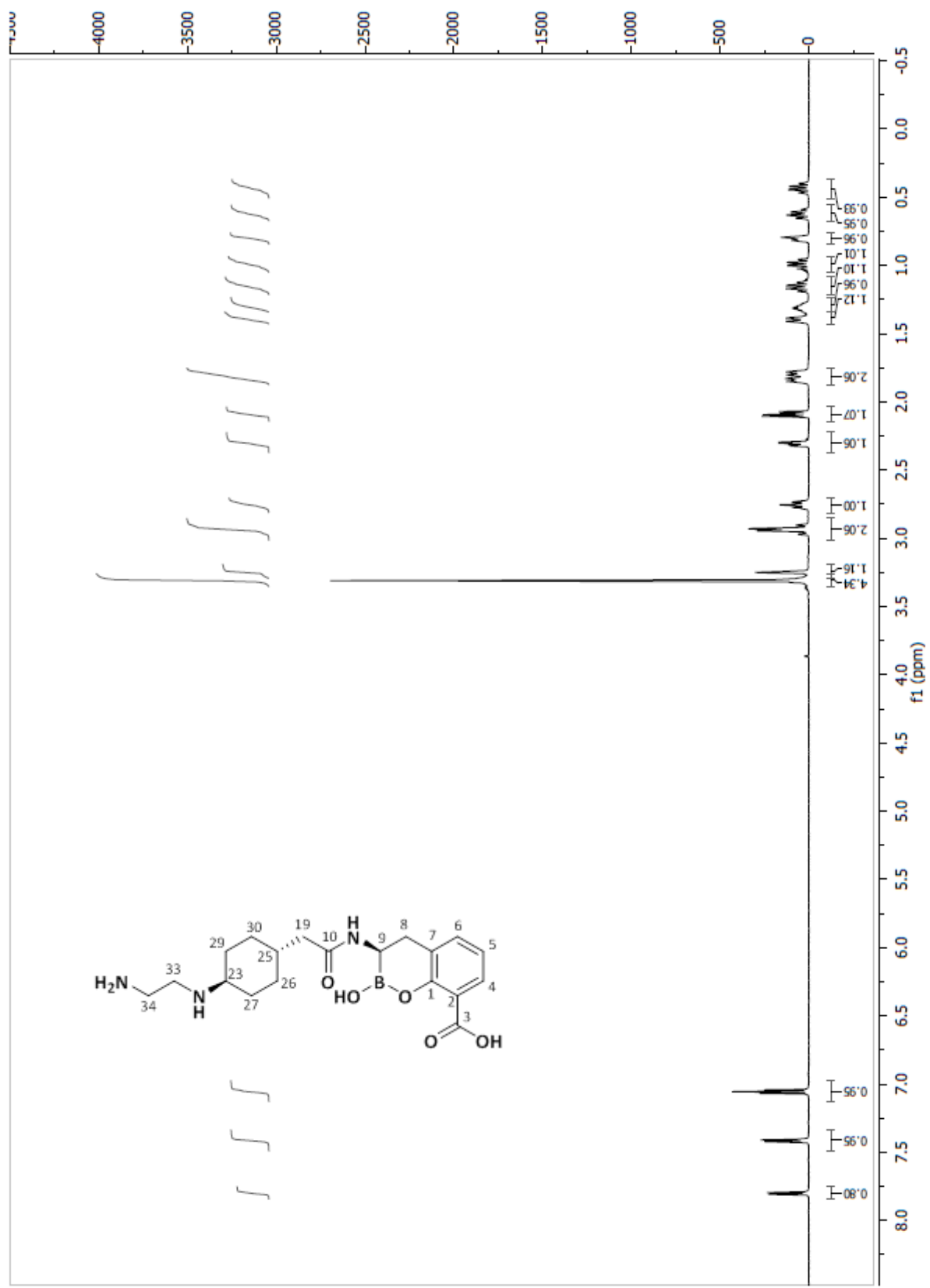


Figure S29. ^1H NMR spectrum of 13 (VNRX-5133)

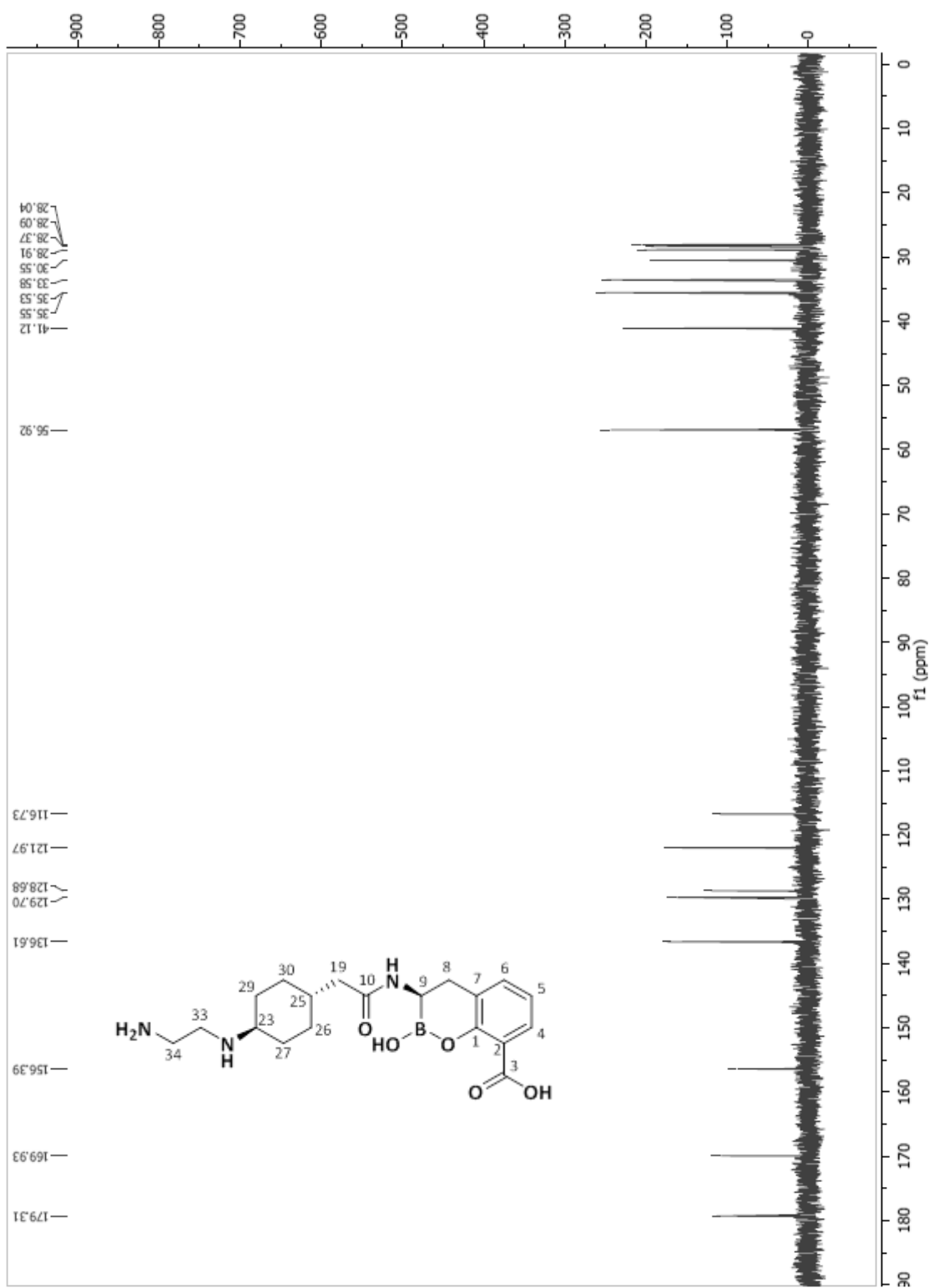


Figure S30. ^{13}C NMR spectrum of 13 (VNRX-5133).

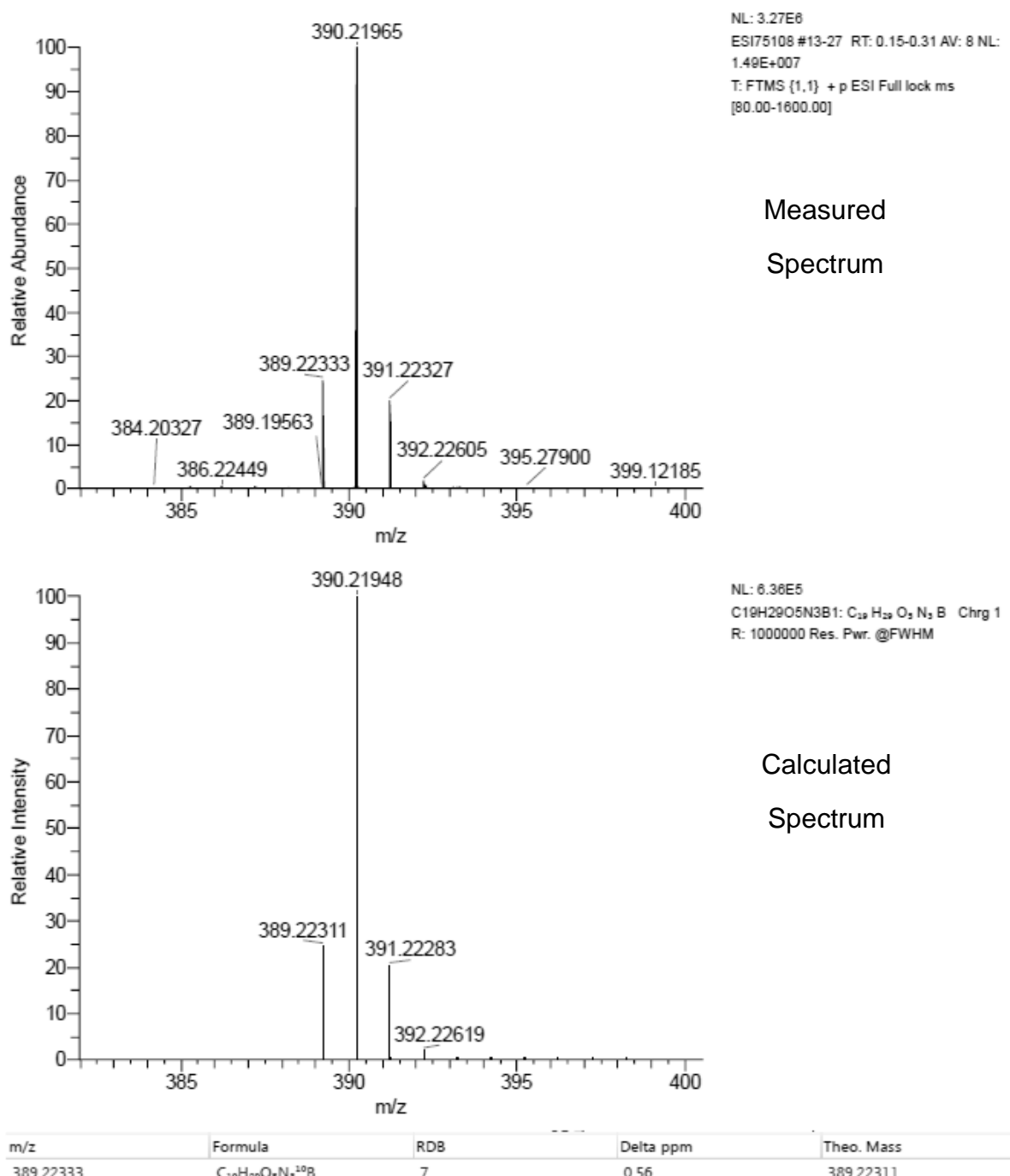


Figure S31. HRMS spectrum of 13 (VNRX-5133).

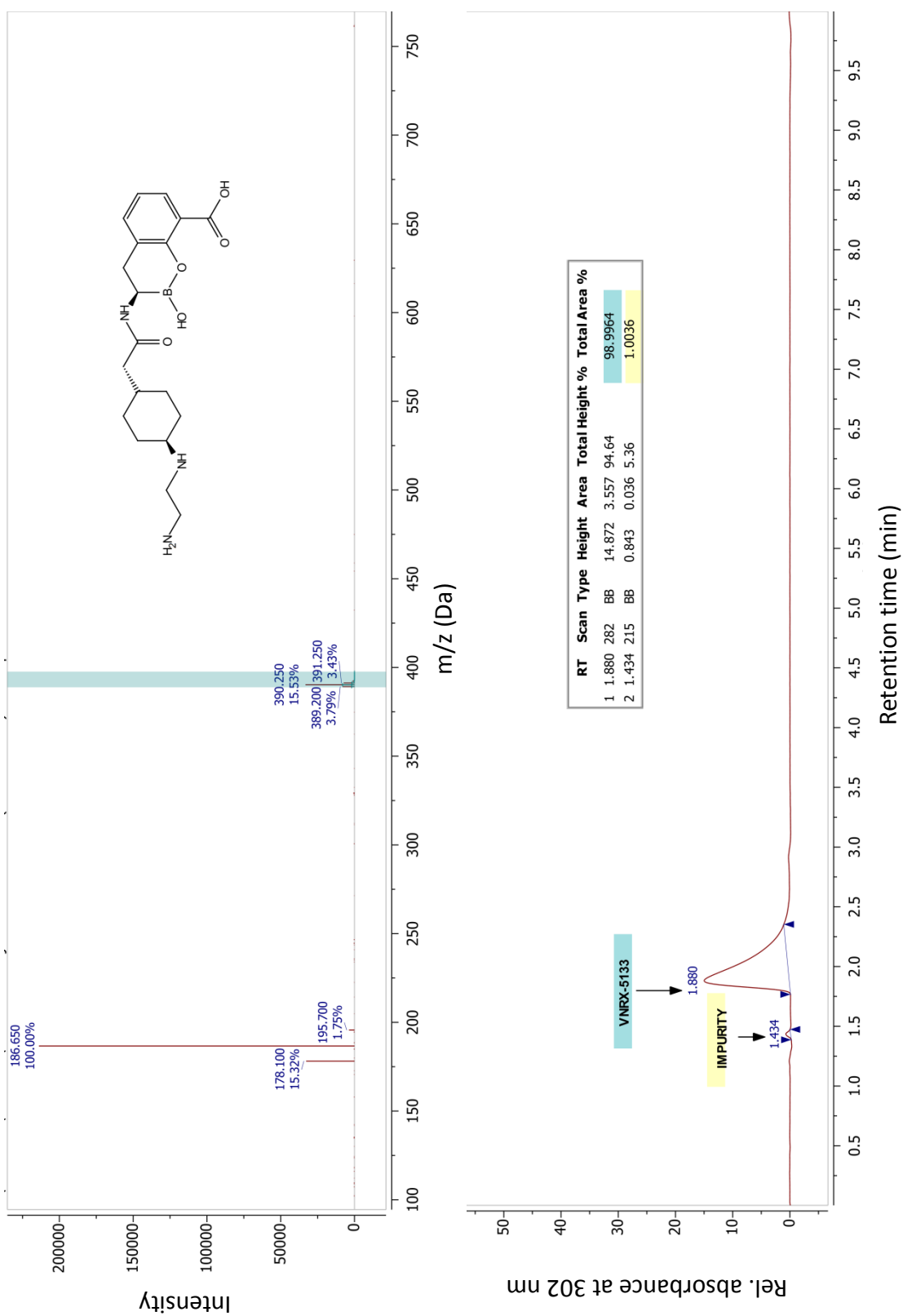


Figure S32. LC-MS spectrum of 13 (VNRX-5133).

Table S1. Error analysis for the obtained inhibition values.

		2,4-DPCA pIC ₅₀ ^a	Std. Error ^b	Captopril pIC ₅₀ ^a	Std. Error ^b	VNRX-5133 pIC ₅₀ ^a	Std. Error ^b
	Class						
SBLs	A	TEM-116	/	/	/	8.9	0.00083
	C	AmpC (<i>P. aeruginosa</i>)	/	/	/	7.52	0.009707
	D	OXA-10	/	/	/	7.63	0.0175
	D	OXA-10 (100 mM NaHCO ₃)	/	/	/	7.19	0.01122
	D	OXA-48	/	/	/	7.27	0.02824
	D	OXA-48 (100 mM NaHCO ₃)	/	/	/	6.62	0.02736
MBLs	B1	VIM-1	/	/	5.1	0.1434	8.1
	B1	NDM-1	/	/	5.0	0.1164	8.0
	B1	VIM-2	/	/	5.8	0.0837 3	9.3
	B1	IMP-1	/	/	5.7	0.0371 6	5.6
	B2	CphA	5.1	0.06257	/	/	5.6
	B3	L1	/	/	/	/	<5.0
^a pIC ₅₀ = -logIC ₅₀ .							
^b Standard logIC ₅₀ errors (Std. Error) were obtained from the GraphPadPrism 6 reports as an average of at least three technical replicates.							
^c NA: pIC ₅₀ value out of range of concentrations tested							

Figure S33. Time course evaluation of pIC₅₀ shifts of VNRX-5133 against subclass B1 MBL NDM-1.

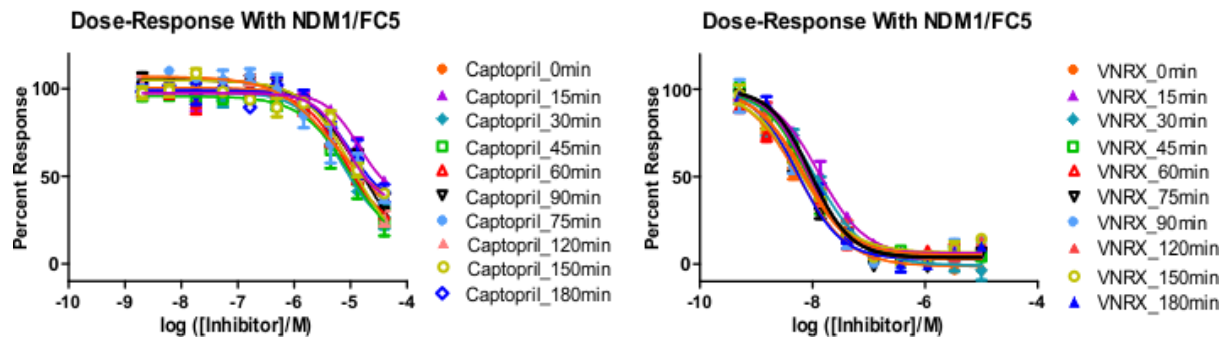


Table S2. Time-dependent inhibition of subclass B1 MBL NDM-1 by VNRX-5133.

Time point (min)	Captopril pIC ₅₀ ^a	Std. Error ^b	VNRX-5133 pIC ₅₀ ^a	Std. Error ^b
0	5.0	0.09623	8.2	0.02657
15	4.8	0.1467	7.9	0.02693
30	5.2	0.1224	7.9	0.05004
45	5.0	0.3054	8.1	0.03735
60	5.1	0.1339	8.2	0.04964
75	5.3	0.3194	8.3	0.03491
90	4.8	0.2977	8.2	0.06285
120	5.0	0.1401	8.1	0.04245
150	5.1	0.1213	8.2	0.04525
180	5.0	0.2465	8.0	0.03313

^a pIC₅₀ = -logIC₅₀.

^b Standard logIC₅₀ errors were obtained from the GraphPadPrism 6 reports as an average of at least three technical replicates.

Table S3. Processing and refinement statistics for NDM-1 / OXA-10 with VNRX-5133.

Data Set	NDM-1:VNRX-5133 complex	OXA-10:VNRX-5133 complex
Beamlne	DLS I24	DLS I03
Space group	$P2_12_12_1$	$P2_12_12_1$
Protein molecules per ASU[†]	2	2
Unit cell dimensions		
<i>a, b, c</i> (Å)	70.82, 73.84, 77.68	48.87, 95.62, 126.26
α, β, γ (°)	90.0, 90.0, 90.0	90.0, 90.0, 90.0
Wavelength(s) (Å)	0.96863	0.97872
Resolution (outer shell) (Å)*	52.34 – 1.51 (1.54 – 1.51)	76.23 – 2.17 (2.21 – 2.17)
R_{pim}	0.103 (1.304)	0.073 (0.261)
CC_{1/2}	0.99 (0.421)	0.9795 (0.8852)
I / σ(I)	8.0 (2.3)	7.89 (3.13)
Completeness (outer shell) (%)	100.0 (100.0)	99.86 (98.96)
Redundancy	11.9 (11.6)	12.50 (12.73)
Refinement		
Resolution (Å)	42.70 – 1.51	63.16 – 2.17 (2.24 – 2.17)
No. reflections	64525	32136 (3141)
R_{work} / R_{free}	0.1456 / 0.1724	20.07 / 22.88
Number of non-hydrogen atoms		
Protein	3472	3816
Solvent	438	304
Zinc ions	4	/
Inhibitor	73	68
B-factors		
Protein	15.90	21.91
Solvent	30.12	28.51
Zn ions	10.73	/
Inhibitor	17.94	25.49
RMSD[‡]		
Ideal bond lengths (Å)	0.009	0.004
Ideal bond angles (°)	0.948	1.00
Ramachandran (%)		
Outliers	0.00	0.00
Favoured	99.12	97.51

ASU[†] = asymmetric unit. RMSD[‡] = root mean square deviation.

*Values in parentheses are for highest-resolution shell.

Table S4. Molprobity validation report for OXA-10:VNRX-5133.

All-Atom Contacts	Clashscore, all atoms:	2.91	100 th percentile * (N=481, 2.17Å ± 0.25Å)	
	<i>Clashscore is the number of serious steric overlaps (> 0.4 Å) per 1000 atoms.</i>			
Protein Geometry	Poor rotamers	1	0.26%	Goal: <0.3%
	Favored rotamers	375	97.15%	Goal: >98%
	Ramachandran outliers	0	0.00%	Goal: <0.05%
	Ramachandran favoured	469	97.51%	Goal: >98%
	MolProbity score [^]	1.16	100 th percentile * (N=10544, 2.17Å ± 0.25Å)	
	Cβ deviations >0.25Å	0	0.00%	Goal: 0
	Bad bonds	2 / 3911	0.05%	Goal: 0%
	Bad angles	0 / 5320	0.00%	Goal: <0.1%
Peptide Omegas	Cis Prolines:	0 / 16	0.00%	Expected: ≤1 per chain, or ≤5%

In the results (3rd and 4th columns), the left column gives the raw count, the right column gives the percentage.

* The 100th percentile is the best among structures of comparable resolution; the 0th percentile is the worst. For the Clashscore the comparative set of structures was selected in 2004, and for the MolProbity score in 2006.

[^] The MolProbity score combines the Clashscore, rotamer, and Ramachandran evaluations into a single score, normalized to be on the same scale as the X-ray structure resolution.

Table S5. Molprobity validation report for NDM-1:VNRX-5133.

All-Atom Contacts	Clashscore, all atoms:	1	99 th percentile * (N=588, 1.510Å ± 0.25Å)	
	<i>Clashscore is the number of serious steric overlaps (> 0.4 Å) per 1000 atoms.</i>			
Protein Geometry	Poor rotamers	4	1.14%	Goal: <0.3%
	Favored rotamers	338	96.02%	Goal: >98%
	Ramachandran outliers	0	0.00%	Goal: <0.05%
	Ramachandran favoured	450	99.12%	Goal: >98%
	MolProbity score [^]	0.84	100 th percentile * (N=4833, 1.510Å ± 0.25Å)	
	Cβ deviations >0.25Å	0	0.00%	Goal: 0
	Bad bonds	0 / 3552	0.00%	Goal: 0%
	Bad angles	1 / 4840	0.02%	Goal: <0.1%
Peptide Omegas	Cis Prolines:	0 / 20	0.00%	Expected: ≤1 per chain, or ≤5%

In the results (3rd and 4th columns), the left column gives the raw count, the right column gives the percentage.

* The 100th percentile is the best among structures of comparable resolution; the 0th percentile is the worst. For the Clashscore the comparative set of structures was selected in 2004, and for the MolProbity score in 2006.

[^] The MolProbity score combines the Clashscore, rotamer, and Ramachandran evaluations into a single score, normalized to be on the same scale as the X-ray structure resolution.

References

1. Baurin, S.; Vercheval, L.; Bouillenne, F.; Falzone, C.; Brans, A.; Jacquemet, L.; Ferrer, J. L.; Sauvage, E.; Dehareng, D.; Frere, J. M.; Charlier, P.; Galleni, M.; Kerff, F. Critical role of tryptophan 154 for the activity and stability of class D beta-lactamases. *Biochem* **2009**, *48*, 11252-11263.
2. King, D. T.; Worrall, L. J.; Gruninger, R.; Strynadka, N. C. New Delhi metallo-beta-lactamase: structural insights into beta-lactam recognition and inhibition. *J Am Chem Soc* **2012**, *134*, 11362-11365.
3. van Berkel, S. S.; Brem, J.; Rydzik, A. M.; Salimraj, R.; Cain, R.; Verma, A.; Owens, R. J.; Fishwick, C. W.; Spencer, J.; Schofield, C. J. Assay platform for clinically relevant metallo-beta-lactamases. *J Med Chem* **2013**, *56*, 6945-6953.
4. Brem, J.; Cain, R.; Cahill, S.; McDonough, M. A.; Clifton, I. J.; Jiménez-Castellanos, J.-C.; Avison, M. B.; Spencer, J.; Fishwick, C. W. G.; Schofield, C. J. Structural basis of metallo- β -lactamase, serine- β -lactamase and penicillin-binding protein inhibition by cyclic boronates. *Nat Commun* **2016**, *7*, 12406.